A 2600-year summer climate reconstruction in central Japan by integrating tree-ring stable oxygen and hydrogen isotopes

Takeshi Nakatsuka[1,2], Masaki Sano[1,3], Zhen Li[1,2], Chenxi Xu[1,4], Akane Tsushima[1], Yuki Shigeoka[2], Kenjiro Sho[5], Keiko Ohnishi[6], Minoru Sakamoto[7], Hiromasa Ozaki[7,8], Noboru Higami[9], Nanae Nakao[10,11], Misao Yokoyama[12] & Takumi Mitsutani[13]

[1] Research Institute for Humanity and Nature, Kyoto 603-8047, Japan.
[2] Graduate School of Environmental Studies, Nagoya University, Nagoya 464-8601, Japan.
[3] Faculty of Human Sciences, Waseda University, Tokorozawa 359-1192, Japan.
[4] Key Laboratory of Cenozoic Geology and Environment, Institute of Geology and Geophysics, Chinese Academy of Sciences, Beijing 100029, China.
[5] Department of Architecture, Civil Engineering and Industrial Management Engineering, Nagoya Institute of Technology, Nagoya 466-8555, Japan.
[6] Institute of Low Temperature Science, Hokkaido University, Sapporo 060-0819, Japan.
[7] National Museum of Japanese History, Sakura 285-8502, Japan.
[8] The University Museum, The University of Tokyo, Tokyo 113-0033, Japan.
[9] Aichi Prefectural Center for Archaeological Operations, Yatomi 498-0017, Japan.
[10] Research Center, Musashi University, Tokyo 176-8534, Japan.
[11] Faculty of Science, Yamagata University, Yamagata 990-8560, Japan.
[12] Graduate School of Agriculture, Kyoto University, Kyoto 606-8502, Japan.
[13] Nara National Research Institute for Cultural Properties, Nara 630-8577, Japan.

Correspondence to: Takeshi Nakatsuka (nakatsuka.takeshi@f.mbox.nagoya-u.ac.jp)

Abstract. Oxygen isotope ratios ($\delta^{18}O$) of tree-ring cellulose are a novel proxy of summer hydroclimate in monsoonal Asia. In central Japan, we collected 67 conifer wood samples, mainly *Chamaecyparis obtusa*, with ages encompassing the past 2,600 yr. The samples were taken from living trees, archaeological wood, architectural wood, and buried logs. We analyzed stable isotope ratios of oxygen ($\delta^{18}O$) and hydrogen ($\delta^{2}H$) in tree-ring cellulose in these samples (more than 15,000 rings in total) without using a pooling method, and constructed a statistically reliable tree-ring cellulose $\delta^{18}O$ time-series for the past 2,500 yr. However, there were distinct age trends and level offsets in the $\delta^{18}O$ record, and cellulose $\delta^{18}O$ values showed a gradual decrease as an individual tree matures. This suggested it is difficult to establish a cellulose $\delta^{18}O$ chronology for low-frequency signals by simple averaging of all the $\delta^{18}O$ time-series data. In addition, there were opposite age trends in the cellulose $\delta^{2}H$, and $\delta^{2}H$ gradually increased with tree age. There were clear positive correlations in the short periodicity variations between $\delta^{18}O$ and $\delta^{2}H$, probably indicating a common climate signal. A comparison of the $\delta^{18}O$ and $\delta^{2}H$ time-series in individual trees with tree-ring width suggested that the opposite age trends of $\delta^{18}O$ and $\delta^{2}H$ are caused by temporal changes in the degree of post-photosynthetic isotope exchange with xylem water (physiological effect), accompanied by changes in stem growth rate that are influenced by human activity in the forests of central Japan. Based on the assumptions that cellulose $\delta^{18}O$ and $\delta^{2}H$ vary positively and negatively with constant proportional coefficients due to climatological and physiological effects,

respectively, we solved simultaneous equations for the climatological and physiological components of variations in tree-ring cellulose $\delta^{18}O$ and δ^2H in order to remove the age trend. This enabled us to evaluate the climatic record from cellulose $\delta^{18}O$ variations. The extracted climatological component in the cellulose $\delta^{18}O$ for the past 2,600 yr in central Japan was well correlated with numerous instrumental, historical, and paleoclimatological records of past summer climate at various spatial and temporal scales. This indicates that integration of tree-ring cellulose $\delta^{18}O$ and δ^2H data is a promising method to reconstruct past summer climate variations on annual to millennial time-scales, irrespective of the growth environment. However, analytical and statistical methods need to be improved for further development of this climate proxy.

1 Introduction

In general, it is not straightforward to extract low-frequency climate signals from tree-ring time-series, because there are typically age trends in tree-ring width. To overcome this, the regional curve standardization (RCS) method is used to determine the typical growth curve in a region for a tree species, which is subtracted from the tree-ring width time-series of individual trees to estimate climatological influences explicitly (Esper et al., 2003), but it is difficult to reserve low-frequency climate signals of tree-ring width/density fully.

Tree-ring cellulose oxygen isotope ratios ($\delta^{18}O$) are a novel proxy of past summer hydroclimate, and it has been reported that such data are not affected by age trends (Young et al., 2011; Kilroy et al., 2016; Xu et al., 2016; Büntgen et al; 2020) or only show short-lived juvenile effects of higher $\delta^{18}O$ values (Szymczak et al., 2012; Duffy et al., 2017). These juvenile effects are interpreted to be related to the less developed root system of young trees and the evaporative enrichment of ^{18}O in soil water in the near-surface. However, Esper et al. (2010) demonstrated the presence of long-term age trends, whereby $\delta^{18}O$ gradually decreases for hundreds of years after germination, as well as significant level offsets between different individual trees, in a conifer species. This requires three analytical criteria to evaluate the age trends and level offsets in the tree-ring cellulose $\delta^{18}O$ data: (1) well-replicated data; (2) non-pooled data; and (3) composite chronologies from multiple species and regions. However, given that subsequent studies of tree-ring cellulose $\delta^{18}O$ have reported that age trends are negligible, the mechanisms responsible for long-term age trends remain unclear.

In Japan, it has been difficult to establish millennial-scale tree-ring chronologies applicable to reconstructing past changes in summer climate, even though such information is critical for rice paddy cultivation and for historical and archaeological studies in Japan. Although there are ancient archaeological and architectural woods that have been used for dendrochronological analysis of wooden artifacts with ages of 1,000–2,000 yr (Mitsutani, 2000; NNRICP, 1990), these have not been utilized for past climate reconstructions. This is because tree-ring widths measured in trees from normal Japanese forests do not have a high sensitivity to climate. Moreover, the ecological and artificial disturbance of tree growth in dense Japanese forests prevents reconstructions of past climate based on the relatively small number of old sub-fossil wood samples that are available.

However, tree-ring cellulose $\delta^{18}O$ data are sensitive to summer hydroclimate in Asia (Treydte et al., 2006; Grießinger et al., 2011; Li et al., 2011; Xu et al., 2011; Sano et al., 2012; Liu et al., 2017), including in Japan (Nakatsuka et al., 2004; Tsuji et al., 2008; Yamaguchi et al., 2010; Li et al., 2015). High correlation coefficients for tree-ring cellulose $\delta^{18}O$ data amongst different individual trees and species make it possible to reconstruct past summer climate using only a small number of sub-fossil trees. Therefore, during the past decade we have analyzed tree-ring cellulose $\delta^{18}O$ in various types of conifer wood with large tree-ring numbers (mainly *Chamaecyparis obtusa*), including from living trees, archaeological wood, architectural wood, and buried logs, in order to reconstruct past variations in summer hydroclimate in central Japan (Nakatsuka, 2015; 2018).

We do not use the pooling method (Szymczak et al., 2012; Loader et al., 2013) for the tree-ring isotope measurements. Instead, we analyze all the tree-rings in the wood samples using a novel method, involving direct cellulose extraction from 1-mm-thick wood sections (Kagawa et al., 2015). This allows us to evaluate age trends in individual trees and offsets between different individuals in the tree-ring cellulose $\delta^{18}O$ data, following the criteria proposed by Esper et al. (2010). This approach has shown that most old trees in Japan (mainly *Chamaecyparis obtusa*) are significantly affected by long-term age trends and level offsets, such that it is not possible to reconstruct long-term summer climate variations without taking these effects into accounts.

However, we have also found that hydrogen isotope ratios (δ^2H) of tree-ring cellulose, which have been measured simultaneously with the $\delta^{18}O$ data, have age trends opposite to those of $\delta^{18}O$, and that δ^2H is positively and negatively correlated with $\delta^{18}O$ in terms of short- and long-periodicity variations, respectively. This $\delta^{18}O$ and δ^2H relationship provides insights into the mechanisms responsible for age trends in tree-ring cellulose $\delta^{18}O$ data, and makes it possible to remove the age trends in such data.

Here, we compare $\delta^{18}O$ and δ^2H data for tree-ring cellulose, and elucidate the mechanisms responsible for age trends in tree-ring cellulose $\delta^{18}O$ data. We then propose and apply a new method to the tree-ring cellulose $\delta^{18}O$ and δ^2H time-series for reconstructing climate over the past 2,600 yr in central Japan. This enables us to remove the age trend and extract the climatological component of the tree-ring cellulose $\delta^{18}O$ data, using many ecologically and artificially disturbed trees that are available for last several thousands of years even in Japan.

2 Samples and chemical analyses

2.1 Collection of tree-ring samples

A total of 67 tree samples covering the past 2,600 yr were collected in central Japan (Fig. 1). These samples consist of living trees, architectural wood, archaeological wood, and buried logs (Table S1). Most of the trees are Japanese cypress (*Chamaecyparis obtusa*), but there are some samples of other conifer species (*Chamaecyparis pisifera*, *Sciadopitys verticillata*, and *Cryptomeria japonica*). All samples contain hundreds of rings. Although some samples have already been dated by traditional dendrochronological methods using tree-ring width (Mitsutani et al., 2000; NNRICP, 1990), the new tree-ring $\delta^{18}O$

time-series were used in the final dendrochronological determination of their ages (Roden, 2008; Yamada et al., 2018), which
100   provided results consistent with the tree-ring width dating results (Fig. S1).

2.2 Measurement of tree-ring cellulose $\delta^{18}O$ and δ^2H

Here, we analyzed cellulose $\delta^{18}O$ and δ^2H for all tree-rings in all wood samples using a novel method, involving direct cellulose extraction from 1-mm-thick wood laths (Kagawa et al., 2015), without using the pooling method. Firstly, 1-mm-thick cross-sectional laths perpendicular to the cellulose fibers were sliced from all wood samples regardless of ring width and age
105   and directly subjected to chemical treatment to remove components other than cellulose. In order to keep original shape of samples during chemical treatments, 1-mm-thick wood laths are put between two Teflon punching sheets and set into test tubes. Given that buried woods sometimes show extraordinary $\delta^{18}O$ values due to alteration of chemical components and/or deposition of iron oxides (Savard et al., 2012; Yapp, 2001), we carefully selected less-degraded wood segments and removed all components other than cellulose completely. A 100–300 µg fragment of cellulose representing the whole annual layer was
110   then cut from the cellulose lath year-by-year using a fine blade under a microscope (Fig. S2). Each sample was wrapped in silver foil for $\delta^{18}O$ and δ^2H measurements using a mass spectrometer combined with a pyrolysis elemental analyzer (TCEA/Delta V Advantage; Thermofisher Scientific, Bremen, Germany). In this study, we analyzed both $\delta^{18}O$ and δ^2H values for each cellulose sample simultaneously by making the focus of mass spectrometer jump automatically between outflows of H_2 and CO gases from pyrolysis elemental analyzer. After measurements of every eight samples, a cellulose standard (cellulose
115   reagent; Merck) with known $\delta^{18}O$ and δ^2H was analyzed to calibrate analytical drift and calculate the $\delta^{18}O$ and δ^2H of samples against the international standard of VSMOW, following Eqs (1) and (2). Analytical reproducibility (1σ) based on repeated measurements of homogeneous cellulose samples is ca. ±0.15‰ and ±1.5‰ for $\delta^{18}O$ and δ^2H, respectively. Absolute accuracies of $\delta^{18}O$ and δ^2H may be a little bit worse because we use only one working standard to minimize the memory effect in δ^2H measurement. However, it does not influence the discussion of this study because we do not utilize absolute isotope
120   values but focus only on their temporal variations.

$$\delta^{18}O_{vsmow}(‰) = \left\{ \frac{\left(^{18}O/^{16}O\right)_{sample}}{\left(^{18}O/^{16}O\right)_{vsmow}} - 1 \right\} \times 1000, \tag{1}$$

$$\delta^2H_{vsmow}(‰) = \left\{ \frac{\left(^2H/^1H\right)_{sample}}{\left(^2H/^1H\right)_{vsmow}} - 1 \right\} \times 1000, \tag{2}$$

Given that cellulose contains 30% of OH-group hydrogen that is exchangeable with experimental water during chemical treatment, it is necessary to remove the OH-group by nitration of the cellulose (synthesis of nitrocellulose) before the isotope
125   measurements (Epstein et al., 1976; DeNiro, 1981). However, it was nearly impossible to nitrate all the cellulose samples

analyzed in this study due to the very small sample amount (Fig. S2) and the extremely large sample number (15,924 rings for isotopic measurements). Moreover, it was desirable to measure both $\delta^{18}O$ and δ^2H simultaneously for each sample, not only for reducing sample number to the half, but also for treating the $\delta^{18}O$ and δ^2H data as those originating from the completely same sample as discussed later, but the nitration of cellulose make it impossible to measure its $\delta^{18}O$ together with δ^2H due to the contamination of oxygen in NO_2-group. However, we can expect that all OH-group hydrogen in a cellulose lath will have a unique δ^2H value, as it would have been replaced by the hydrogen of homogeneous water in the test tube during the process of cellulose extraction, such that the measured tree-ring cellulose δ^2H time-series will retain the original isotopic variations, although the amplitude of these variations will decrease by up to 70% and the absolute values will have been modified (Filot et al., 2006). We confirmed that there are consistent correlations in δ^2H variations between cellulose and nitrocellulose produced using the traditional nitration method (Epstein et al., 1976; DeNiro, 1981) for two tree samples (Fig. 2), although the correlation coefficients are lower than that by a more sophisticated method to fix δ^2H value of OH-group in cellulose (Filot et al., 2006). This demonstrates that it is possible to reconstruct original variations in tree-ring cellulose δ^2H data without nitrating the cellulose to a certain degree. However, considering the possible analytical uncertainties in cellulose δ^2H data of this study, we restrict the usage of δ^2H data just to calibration of long-term age trends in cellulose $\delta^{18}O$ as discussed later.

3 Results and Discussion

3.1 Variations in the tree-ring cellulose $\delta^{18}O$ and δ^2H data

After constraining the exact dates for all the tree-rings by the cross-dating method using $\delta^{18}O$ data (Fig. S1), we compared all tree-ring cellulose $\delta^{18}O$ and δ^2H time-series (Fig. 3a and c).

Given that the average correlation coefficient (R-bar) amongst the different $\delta^{18}O$ time-series is ca. 0.6–0.8, the Expressed Population Signal (EPS) (Wigley et al., 1984), defined as $N \times R/[1 + (N - 1) \times R]$ where the N and R values are the number of time-series and R-bar respectively, is >0.85 for almost all periods during the past 2,500 yr (Fig. 3b), indicating that the $\delta^{18}O$ data in Fig. 3a are sufficient to establish accurate $\delta^{18}O$ chronologies. However, there are distinct long-term age trends, in that the $\delta^{18}O$ values gradually decrease as the trees mature, as also noted by Esper et al. (2010). These effects must be detrended in order to reconstruct long-term climate variations using the $\delta^{18}O$ data. There are also significant offsets in absolute $\delta^{18}O$ values for each year amongst different trees, probably reflecting differences in the sample location and magnitude of the age trend. Given the original locations of the trees cover a wide region from coastal to inland areas and low to high altitudes (Fig. 1), this would result in different precipitation $\delta^{18}O$ values and relative humidity (Waseda and Nakai, 1983; Araguás-Araguás et al., 2000; Shu et al., 2005). This would account for the offset absolute $\delta^{18}O$ values of tree-ring cellulose in different trees.

R-bar for the different δ^2H time-series is ca. 0.2–0.4, resulting in lower EPS values (Fig. 3d), which must reflect more complicated post-photosynthetic changes of isotopic ratios in hydrogen than in oxygen (Roden et al., 2000) as discussed later,

but may be partly owing to the analytical uncertainty by the direct measurement of cellulose hydrogen including the OH-group in the δ^2H measurements. However, there are also distinct age trends, which are opposite to those exhibited by δ^{18}O, in that δ^2H values gradually increase as the trees mature.

3.2 Relationship between short- and long-periodicity δ^{18}O and δ^2H variations

160   To investigate the environmental causes of the age trends in tree-ring cellulose δ^{18}O and δ^2H data, we decomposed the δ^{18}O and δ^2H time-series into short- and long-periodicity variations (Figs 4 and S3, S4, S5). These trees (No. 65 and No. 43, 49, 40; Table S1) are Japanese cypress (*Chamaecyparis obtusa*) from Nagano and Gifu Prefectures. In all cases, short-periodicity variations (i.e., <11 yr) in the tree-ring cellulose δ^{18}O and δ^2H data show a clear positive correlation, indicating that both the δ^{18}O and δ^2H variations reflect a common climatological signal (i.e., precipitation isotope ratios and relative

165   humidity) as reported in previous studies (e.g., An et al., 2014). However, the long-periodicity variations (i.e., >11 yr) in the tree-ring cellulose δ^{18}O and δ^2H data show negative correlations (Figs 4b and S3b), suggesting the influence of opposite age trends in Fig. 3. However, the negative correlations are not very clear in Figs S4b and S5b, probably because the climatological signals also overlap the long-periodicity variations and make the correlation between the tree-ring cellulose δ^{18}O and δ^2H positive to a certain degree.

170   Figures 4b and S3b, S4b, S5b show that δ^{18}O and δ^2H often changed oppositely in the long-periodicity variations, regardless of the tree age. Therefore, the long-term opposite variations in the tree-ring cellulose δ^{18}O and δ^2H data are not a simple age trend. As such, it is impossible to apply the RCS or negative exponential curve proposed by Esper et al. (2010) for removing the apparent age trend of tree-ring cellulose δ^{18}O in central Japan.

        To date, the age trend in tree-ring cellulose δ^{18}O data has been explained by the relatively shallow root system of juvenile

175   trees and the evaporative enrichment of ^{18}O in soil water at the near-surface. However, this cannot explain the long-term variations in tree-ring cellulose δ^{18}O and δ^2H data in this study (Figs 4 and S3, S4, S5), because the soil water evaporation must increase both δ^{18}O and δ^2H. As illustrated in Supplement A and Fig. S6, the long-term opposite variations in tree-ring cellulose δ^{18}O and δ^2H are tightly related to changes in tree-ring with (growth rate of trees), suggesting that they are influenced by some physiological effect corresponding to long-term changes in tree growth rate.

180 ### 3.3 Mechanical model of cellulose δ^{18}O and δ^2H

        What physiological mechanism can explain the long-term opposite variations in the δ^{18}O and δ^2H values? Tree-ring cellulose δ^{18}O and δ^2H values can be expressed using the following equations, which are modified and simplified from Roden et al. (2000):

$$\delta^{18}O_{cel} = f\,(\delta^{18}O_{rain} + \varepsilon_{ho}) + (1-f)[\delta^{18}O_{rain} + (\varepsilon_{eo} + \varepsilon_{ko})(1-h) + \varepsilon_{ao}], \tag{3}$$

185 $\delta^2H_{cel} = f(\delta^2H_{rain} + \varepsilon_{hh}) + (1-f)[\delta^2H_{rain} + (\varepsilon_{eh} + \varepsilon_{kh})(1-h) + \varepsilon_{ah}]$,   (4)

where cel and rain indicate the tree-ring cellulose and precipitation, respectively; h is the relative humidity during photosynthesis; f is the proportion of oxygen atoms in carbohydrate exchanged with xylem water during post-photosynthetic processes before cellulose synthesis, which is assumed to be equal to that of the hydrogen atoms; ε_{eo} (ε_{eh}) and ε_{ko} (ε_{kh}) are isotopic fractionation factors for oxygen (hydrogen) during equilibrium evaporation between water and water vapor and kinetic 190 water vapor diffusion through leaf stomata, respectively; and ε_{ao} (ε_{ah}) and ε_{ho} (ε_{hh}) are isotopic fractionation factors for oxygen (hydrogen) between water and carbohydrate during photosynthesis in the leaf and the post-photosynthetic processes before cellulose synthesis, respectively. Values of ε_{eo}, ε_{ko}, ε_{ao}, and ε_{ho} are +9, +29, +27, and +27, respectively, while ε_{eh} and ε_{kh} are +80 and +25, respectively, and ε_{ah} and ε_{hh} are approximately –150 and +150, respectively (Roden et al., 2000).

Given that we can assume that all the isotopic fractionation factors are constant, $\delta^{18}O_{cel}$ and δ^2H_{cel} are determined only by 195 climatological factors ($\delta^{18}O_{rain}$, δ^2H_{rain}, and h) when f is constant. Because there are always positive correlations between $\delta^{18}O_{rain}$ and δ^2H_{rain} (Dansgaard, 1964) and any change of h produces changes in $\delta^{18}O_{cel}$ and δ^2H_{cel} in Eqs (3) and (4) in the same direction, we can expect that there are also positive correlations between $\delta^{18}O_{cel}$ and δ^2H_{cel} when f is constant. In fact, even in trees that have negative correlations between $\delta^{18}O_{cel}$ and δ^2H_{cel} for the long-periodicity variations, we observe clear positive correlations in the short-periodicity variations (Figs 4c and S3c, S4c, S5c), suggesting that f does not change on annual time- 200 scales and the short-periodicity variations in $\delta^{18}O_{cel}$ and δ^2H_{cel} are controlled solely by climatological factors.

However, if f increases over the long-term due to some physiological reason, it can be inferred from Eqs (3) and (4) that $\delta^{18}O_{cel}$ decreases while δ^2H_{cel} increases. This is because, for oxygen, the magnitude of isotopic fractionation between water and carbohydrate is the same (+27) for photosynthesis (ε_{ao}) and post-photosynthesis processes (ε_{ho}), and the increase in f reduces the effect of leaf water ^{18}O enrichment, $(\varepsilon_{Oe} + \varepsilon_{Ok})(1-h)$ in Eq. (3), resulting in lower $\delta^{18}O_{cel}$. However, for hydrogen, 205 the magnitude of isotopic fractionation between water and carbohydrate during post-photosynthesis processes ($\varepsilon_{hh} = +150$) is significantly larger than that during photosynthesis ($\varepsilon_{ah} = –150$), such that the increase in f results in higher δ^2H_{cel}. This causes long-term opposite trends in $\delta^{18}O_{cel}$ and δ^2H_{cel} data (Figs 3, 4b, and S3b, S4b, S5b), which can be interpreted as a long-term change in the rate of post-photosynthetic isotopic exchange between carbohydrate and xylem water (f). Possible physiological mechanisms for this include an increase in the rate of utilization of stored carbohydrates for stem cellulose synthesis 210 (Nabeshima et al., 2018), rather than using photosynthetic products directly for rapid tree growth during the juvenile period. The change in f value could also occur in the period following an abrupt improvement in the growth environment, due to logging of neighboring trees (see Supplement A and Fig. S6).

Although the long-periodicity variations in $\delta^{18}O_{cel}$ and δ^2H_{cel} are influenced by predominant physiological effects (Figs 4b and S3b, S4b, S5b), this does not mean that the long-periodicity variations in $\delta^{18}O_{cel}$ and δ^2H_{cel} do not contain climatological 215 components. In fact, climate varies at all time-scales, such that long-term variations in $\delta^{18}O_{cel}$ and δ^2H_{cel} inevitably include

climatological components. It is therefore challenging to resolve the climatic signals from the physiological effects. In dendrochronological studies based on tree-ring width, RCS is used to separate and estimate climatological components in tree-ring width time-series (Esper et al., 2002; Grudd et al., 2002; Büntgen et al., 2005). However, it is difficult to create a regional standardized $\delta^{18}O_{cel}$ curve like the RCS for the samples analyzed in this study, because the physiological effects on $\delta^{18}O_{cel}$ are

220   not solely an age trend, and also reflect past human disturbances to the trees such as logging activity (see Supplement A).

3.4 Classification of $\delta^{18}O$ and δ^2H variations into climatological and physiological components

To extract the climatological component of the variations in the tree-ring cellulose $\delta^{18}O$ data, we modified the model of cellulose $\delta^{18}O$ and δ^2H in Eqs (3) and (4) into climatological and physiological components. Given there are four variables ($\delta^{18}O_{rain}$, δ^2H_{rain}, h, and f) in Eqs (3) and (4), we first define their variations as follows:

225
$$\delta^{18}O_{rain} = \delta^{18}O_{rain(0)} + \Delta\delta^{18}O_{rain}, \tag{5}$$

$$\delta^2H_{rain} = \delta^2H_{rain(0)} + \Delta\delta^2H_{rain}, \tag{6}$$

$$h = h_{(0)} + \Delta h, \tag{7}$$

$$f = f_{(0)} + \Delta f, \tag{8}$$

where $\delta^{18}O_{rain(0)}$, $\delta^2H_{rain(0)}$, $h_{(0)}$, and $f_{(0)}$ are $\delta^{18}O_{rain}$, δ^2H_{rain}, h, and f in a fixed year (0), respectively, and $\Delta\delta^{18}O_{rain}$, $\Delta\delta^2H_{rain}$, Δh,

230   and Δf are deviations in $\delta^{18}O_{rain}$, δ^2H_{rain}, h, and f from the fixed year (0) to an arbitrary year, respectively. By substituting Eqs (5)–(8) into Eqs (3)–(4) and neglecting the second-order minor terms ($\Delta f\Delta h$, $\Delta f\Delta\delta^{18}O_{rain}$, and $\Delta f\Delta\delta^2H_{rain}$), Eqs (3) and (4) can be rewritten as follows:

$$\delta^{18}O_{cel} = f_{(0)}\left(\delta^{18}O_{rain(0)} + \varepsilon_{ho}\right) + \left(1 - f_{(0)}\right)\left[\delta^{18}O_{rain(0)} + (\varepsilon_{eo} + \varepsilon_{ko})\left(1 - h_{(0)}\right) + \varepsilon_{ao}\right]$$
$$+ \left[\Delta\delta^{18}O_{rain} - \Delta h(\varepsilon_{eo} + \varepsilon_{ko})\left(1 - f_{(0)}\right)\right]$$

235
$$+ \Delta f\left[\varepsilon_{ho} - \varepsilon_{ao} - (\varepsilon_{eo} + \varepsilon_{ko})\left(1 - h_{(0)}\right)\right], \tag{9}$$

$$\delta^2H_{cel} = f_{(0)}\left(\delta^2H_{rain(0)} + \varepsilon_{hh}\right) + \left(1 - f_{(0)}\right)\left[\delta^2H_{rain(0)} + (\varepsilon_{eh} + \varepsilon_{kh})\left(1 - h_{(0)}\right) + \varepsilon_{ah}\right]$$
$$+ \left[\Delta\delta^2H_{rain} - \Delta h(\varepsilon_{eh} + \varepsilon_{kh})\left(1 - f_{(0)}\right)\right]$$
$$+ \Delta f\left[\varepsilon_{hh} - \varepsilon_{ah} - (\varepsilon_{eh} + \varepsilon_{kh})\left(1 - h_{(0)}\right)\right]. \tag{10}$$

We can now introduce new equations for the climatological and physiological components in the tree-ring cellulose $\delta^{18}O$

240   and δ^2H time-series, as follows:

$$\Delta\delta^{18}O_{cel(climate)} = \Delta\delta^{18}O_{rain} - \Delta h(\varepsilon_{eo} + \varepsilon_{ko})(1 - f_{(0)}), \tag{11}$$

$$\Delta\delta^{2}H_{cel(climate)} = \Delta\delta^{2}H_{rain} - \Delta h(\varepsilon_{eh} + \varepsilon_{kh})(1 - f_{(0)}), \tag{12}$$

$$\Delta\delta^{18}O_{cel(physiol)} = \Delta f[\varepsilon_{ho} - \varepsilon_{ao} - (\varepsilon_{eo} + \varepsilon_{ko})(1 - h_{(0)})], \tag{13}$$

$$\Delta\delta^{2}H_{cel(physiol)} = \Delta f[\varepsilon_{hh} - \varepsilon_{ah} - (\varepsilon_{eh} + \varepsilon_{kh})(1 - h_{(0)})], \tag{14}$$

245   where $\Delta\delta^{18}O_{cel(climate)}$, $\Delta\delta^{18}O_{cel(physiol)}$, $\Delta\delta^{2}H_{cel(climate)}$, and $\Delta\delta^{2}H_{cel(physiol)}$ are variations in the tree-ring cellulose $\delta^{18}O$ and $\delta^{2}H$ from the fixed year (0) with respect to an arbitrary year due to climatological and physiological factors, respectively. We can then reformulate $\delta^{18}O_{cel}$ and $\delta^{2}H_{cel}$ as the sum of climatological and physiological components, as follows:

$$\delta^{18}O_{cel} = \delta^{18}O_{cel(0)} + \Delta\delta^{18}O_{cel(climate)} + \Delta\delta^{18}O_{cel(physiol)}, \tag{15}$$

$$\delta^{2}H_{cel} = \delta^{2}H_{cel(0)} + \Delta\delta^{2}H_{cel(climate)} + \Delta\delta^{2}H_{cel(physiol)}, \tag{16}$$

250   where $\delta^{18}O_{cel(0)}$ and $\delta^{2}H_{cel(0)}$ are $\delta^{18}O_{cel}$ and $\delta^{2}H_{cel}$ at the fixed year (0), respectively.

3.5 A method to extract the climatological component from cellulose $\delta^{18}O$

     Here we propose a new method to calculate the climatological component in variations of the tree-ring cellulose $\delta^{18}O$ ($\Delta\delta^{18}O_{cel(climate)}$) by solving simultaneous equations consisting of Eqs (15)–(16), with two additional equations based on the relationship between $\Delta\delta^{18}O_{cel(climate)}$ and $\Delta\delta^{2}H_{cel(climate)}$ and between $\Delta\delta^{18}O_{cel(physiol)}$ and $\Delta\delta^{2}H_{cel(physiol)}$ (i.e., Eqs (17)–(18)).
255   This is based on the theoretical and observational understanding that tree-ring cellulose $\delta^{18}O$ and $\delta^{2}H$ data correlate positively and negatively due to climatological and physiological factors, respectively. (Note that we restrict the physiological effects to the change in rate of post-photosynthesis isotope exchange with xylem water here. If there are other types of ecophysiological effects generating a positive relationship between $\delta^{18}O_{cel}$ and $\delta^{2}H_{cel}$ such as the root deepening or growth season shift, they are counted as parts of climatological effects here.)

260
$$\Delta\delta^{2}H_{cel(climate)} = A \times \Delta\delta^{18}O_{cel(climate)}, \tag{17}$$

$$\Delta\delta^{2}H_{cel(physiol)} = -B \times \Delta\delta^{18}O_{cel(physiol)}, \tag{18}$$

where A and B are positive proportional coefficients, as shown in Eqs (19)–(20) and defined by Eqs (11)–(14).

$$A = \frac{\Delta\delta^2H_{rain} - \Delta h(\varepsilon_{eh} + \varepsilon_{kh})(1 - f_{(0)})}{\Delta\delta^{18}O_{rain} - \Delta h(\varepsilon_{eo} + \varepsilon_{ko})(1 - f_{(0)})}, \tag{19}$$

$$B = -\frac{\varepsilon_{hh} - \varepsilon_{ah} - (\varepsilon_{eh} + \varepsilon_{kh})(1 - h_{(0)})}{\varepsilon_{ho} - \varepsilon_{ao} - (\varepsilon_{eo} + \varepsilon_{ko})(1 - h_{(0)})}, \tag{20}$$

265   If A and B are constant, we can solve the simultaneous equations (15)–(18) in order to cancel out the physiological component ($\Delta\delta^{18}O_{cel(physiol)}$) and extract the climatological component ($\Delta\delta^{18}O_{cel(climate)}$), as follows:

$$\Delta\delta^{18}O_{cel(climate)} = \frac{\delta^2H_{cel} + B \times \delta^{18}O_{cel}}{A + B} - \frac{\delta^2H_{cel(0)} + B \times \delta^{18}O_{cel(0)}}{A + B}, \tag{21}$$

In fact, A might not be constant because there are three variables ($\Delta\delta^{18}O_{rain}$, $\Delta\delta^2H_{rain}$, and Δh) in Eq. (19). $\Delta\delta^{18}O_{rain}$ and $\Delta\delta^2H_{rain}$ may change somewhat independently from each other over a wide spatiotemporal range, and the relationship between

270    $\Delta\delta^{18}O_{rain}$ ($\Delta\delta^2H_{rain}$) and Δh may not be simple in Eq. (19). However, the significant positive correlations in the short-periodicity variations between $\delta^{18}O_{cel}$ and δ^2H_{cel} (Figs 4c and S3c, S4c, S5c) suggest there may be an empirical constant value for A in a restricted study area such as central Japan. In contrast to A, B may be nearly constant because there are no variables in Eq. (20).

Although the assumption that A and B are constant might not be valid, this assumption is needed to explicitly calculate

275    $\Delta\delta^{18}O_{cel(climate)}$ using Eq. (21). Hence, we tentatively assumed that A and B are constant, and calculated $\Delta\delta^{18}O_{cel(climate)}$ over the past 2,600 yr using Eq. (21). We then verify this by comparison with numerous local, regional, and global meteorological, historical, and paleoclimatological records of past summer climate over various time-scales, in order to judge whether the simplest assumption, that A and B in Eq (21) are constant, is practically useful or not for paleoclimatological studies.

3.6 Method to determine the proportional coefficients A and B

280   To utilize Eq. (21), we need to determine the proportional coefficients A and B in Eqs (17)–(20). In principle, there are two ways to determine A and B: a theoretical approach based on Eqs (19)–(20), and an empirical approach based on Eqs (17)–(18).

We first consider the feasibility of the theoretical approach. It is not easy to determine A using Eq. (19), because there are three variables ($\Delta\delta^{18}O_{rain}$, $\Delta\delta^2H_{rain}$, and Δh). If the rainwater isotope ratios do not change (both $\Delta\delta^{18}O_{rain}$ and $\Delta\delta^2H_{rain} = 0$), then

285   A is equal to ($\varepsilon_{eh} + \varepsilon_{kh}$)/($\varepsilon_{eo} + \varepsilon_{ko}$), which is (80 + 25)/(9 + 29) = 2.76 (Roden and Ehleringer, 2000). However, if relative humidity does not change ($\Delta h = 0$), A = $\Delta\delta^2H_{rain}$ /$\Delta\delta^{18}O_{rain}$, which is equal to 8 if the meteoric water line is followed (Dansgaard, 1964). Given the wide range of potential A values from 2.76 to 8, we cannot easily theoretically define A. On the other hand,

B may be easier to determine theoretically, because there are no variables in Eq. (20). For example, if the relative humidity $h_{(0)}$ is 0.5, B = 13 because ε_{eo}, ε_{ko}, ε_{ao}, ε_{ho}, ε_{eh}, ε_{kh}, ε_{ah}, and ε_{hh} are +9, +29, +27, +27, +80, +25, ca. –150, and +150, respectively
290 (Roden et al., 2000). However, in fact, it is not easy to fix $h_{(0)}$ because the relative humidity typically shows large diurnal variations, and the timing of $\delta^{18}O$ incorporation into leaf carbohydrate is unknown. Moreover, the ε_{ah} and ε_{hh} values of –150 and +150 are just approximations. For example, while Yakir and DeNiro (1990) obtained values of –171 and +158 for ε_{ah} and ε_{hh}, respectively, Estep and Hoering (1981) obtained values of –100 to –120 for ε_{ah} and Luo and Sternberg (1992) reported values of +144 to +166 for ε_{hh}.

295   Therefore, we used the empirical approach for estimating A and B. The A value in Eq. (17) can be estimated from the relationship between $\delta^{18}O_{cel}$ and δ^2H_{cel} in the short-periodicity variations, because they are positively correlated due to the climate variations shown in Figs 4c and S3c, S4c, S5c. In the case of the B value in Eq. (18), the situation is more complex. Although there are apparent negative correlations between $\delta^{18}O_{cel}$ and δ^2H_{cel} in the long-periodicity variations (Figs 4b and S3b), these are also affected by long-term climate signals, such that it is difficult to resolve the physiological component. Here
300 we propose a practical method to determine the B value. After fixing A, we first set various B values in order to calculate the temporal variations in the climatological component of the tree-ring cellulose $\delta^{18}O$ data ($\Delta\delta^{18}O_{cel(climate)}$) for all 67 tree samples, by substituting individual $\delta^{18}O_{cel}$ and δ^2H_{cel} time-series in Fig. 3a and 3c into Eq. (21). We then combine the $\Delta\delta^{18}O_{cel(climate)}$ time-series of all 67 trees calculated from each B value using the method described below (Sect. 3.7). Finally, we compare the overall trend of the combined time-series of $\Delta\delta^{18}O_{cel(climate)}$ data with that of a simple average of all 67 raw $\delta^{18}O_{cel}$ time-series
305 in Fig. 3a, in order to find the B value that produced the best match between the two time-series. This procedure assumes that, although individual trees possess different age trends and level offsets, averaging of all data from all trees covering all periods and all locations in this study may cancels out these effects and allows climate variations to be discerned, at least in terms of "the overall trend".

3.7 Method to combine individual tree-ring time-series with large level offsets

310   To reconstruct multi-millennial variations in the climatological component of the tree-ring cellulose $\delta^{18}O$ data ($\Delta\delta^{18}O_{cel(climate)}$), we must combine individual time-series from different trees with variable level offsets due to different sample locations. As such, we cannot simply average all data for individual trees, because this produces steps in the composite record at both ends of the time-series of individual trees. Numerous procedures have been proposed to combine tree-ring time-series (e.g., Hangartner et al., 2012); here we propose a new iterative calculation method (Fig. 5).
315   Firstly, we simply average all the individual time-series to make a preliminary combined time-series. Secondly, we offset each individual time-series up or down, retaining their original patterns of temporal variations, to the position where the temporal average of the individual time-series becomes equal to that of the preliminary combined time-series for the corresponding period of the individual tree. Thirdly, we average all the offsetted individual time-series to make a refined combined time-series. We iterate this procedure until the temporal average of the individual time-series becomes equal to that

320 of the combined time-series for the corresponding period, without any further offsetting of the individual time-series. If you start from the same original dataset on $\delta^{18}O$ variations of stem segments, the pattern of relative variation in the final combined $\delta^{18}O$ time-series is mathematically unique although its absolute value has no meaning. That is, there is no room where some artefact influences resultant time-series. This method assumes that the tree-ring absolute isotope ratios of individual trees are not important, because they depend on the sample locations, but that the temporal variations are well correlated amongst

325 different trees due to a common regional climate signal.

3.8 Procedure to calculate the climatological component in tree-ring $\delta^{18}O$ ($\Delta\delta^{18}O_{cel(climate)}$) data

Figure 6a shows how the combined time-series for $\Delta\delta^{18}O_{cel(climate)}$ is constructed. Firstly, we determine A from the short-periodicity variations between $\delta^{18}O_{cel}$ and δ^2H_{cel} in individual trees. Secondly, we use $\delta^{18}O_{cel}$ and δ^2H_{cel} to calculate $\Delta\delta^{18}O_{cel(climate)}$ for individual trees using various B values in Eq. (21). Thirdly, we combine the $\Delta\delta^{18}O_{cel(climate)}$ time-series of all

330 trees for each case of different B values. Fourthly, we select the best B value by comparison of the overall trends in the combined $\Delta\delta^{18}O_{cel(climate)}$ and average $\delta^{18}O_{cel}$ data. Finally, we reintegrate the long-periodicity variations in $\Delta\delta^{18}O_{cel(climate)}$ calculated using the best B value and short-periodicity variations in $\delta^{18}O_{cel}$ for all individual trees at an adequate threshold periodicity and combine all individual data again, because the physiological factors do not appear to affect the short-periodicity $\delta^{18}O_{cel}$ variation so that we should keep the original $\delta^{18}O_{cel}$ variations in the high-frequency domain. In this procedure (Fig.

335 6a), the iterative calculation used to combine many tree-ring time-series in the third step is the most time-consuming because various B values are tested.

Although A can be determined independently for each tree, we can only obtain one B value for all the trees. In a practical sense, it is not meaningful to determine A separately for each tree, because all the trees were collected within central Japan (Fig. 1). If we assume that A and B are unique for all trees in this study, we can simplify the procedure as shown in Fig. 6b to

340 reduce the time required for the iterative calculation. Considering that all the calculations used to combine and integrate the time-series in Fig. 6 are linear, we can change the order of calculation between combination and integration. In fact, if we use common A and B values, the resultant combined time-series for $\Delta\delta^{18}O_{cel(climate)}$ does not change when using the two procedures (Fig. 6a and b). In Fig. 6b, we first combine the $\delta^{18}O_{cel}$ and δ^2H_{cel} time-series of all trees in Fig. 3, using the method shown in Fig. 5. Secondly, we determine A by investigating the relationship between short-periodicity variations of $\delta^{18}O_{cel}$ and δ^2H_{cel} in

345 their combined time-series. Thirdly, we integrate the combined $\delta^{18}O_{cel}$ and δ^2H_{cel} records to show temporal variations in $\Delta\delta^{18}O_{cel(climate)}$ using various B values. Fourthly, we select the best B value by comparison of the overall trends of the $\Delta\delta^{18}O_{cel(climate)}$ time-series and average $\delta^{18}O_{cel}$. Finally, we reintegrate the long-periodicity variations in $\Delta\delta^{18}O_{cel(climate)}$ and short-periodicity variations in combined $\delta^{18}O_{cel}$ at an adequate threshold periodicity to keep the original $\delta^{18}O_{cel}$ variation in the high-frequency domain.

350 ### 3.9 Determination of the climatological and physiological proportional coefficients (A and B)

We combined all the time-series for $\delta^{18}O_{cel}$ and δ^2H_{cel} shown in Fig. 3 using the method illustrated in Fig. 5. The final combined $\delta^{18}O_{cel}$ and δ^2H_{cel} time-series after 1000 iterations are shown in Fig. 7. The long-term variations in the combined $\delta^{18}O_{cel}$ and δ^2H_{cel} time-series obviously reflect the accumulated age trends, in which the $\delta^{18}O_{cel}$ and δ^2H_{cel} tend to decrease and increase over a long time-scale, respectively.

355   We found that the climatological proportional coefficient A in Eq. (17) can be set to 5, because there are positive correlations in the short-periodicity variations of the combined δ^2H_{cel} and $\delta^{18}O_{cel}$ records with a slope of ca. 5 (Fig. 8), irrespective of the threshold year for extracting the short-periodicity variations (i.e., 5, 11, or 21 yr). A value of 5 is within the theoretical range of A of 2.76 to 8 obtained from Eq. (19). We used the δ^2H_{cel} data directly for the calculation of A, although the amplitude of variations in δ^2H_{cel} is reduced to 70% of that of the original cellulose, such that a value of 5 is equivalent to 360   about 7 in the theoretical range.

  To determine the most appropriate value for the physiological proportional coefficient B in Eq. (18), we integrated the combined $\delta^{18}O_{cel}$ and δ^2H_{cel} time-series in Fig. 9 using Eq. (21), in order to calculate $\Delta\delta^{18}O_{cel(climate)}$ with B values of 3, 5, 7, and 9, and an A value 5. We then examined the overall trend in $\Delta\delta^{18}O_{cel(climate)}$ and found that it became equal to the overall trend of the average $\delta^{18}O_{cel}$ (Fig. 3a), when B = 5.4 (Fig. 9). Given the 70% amplitude reduction of $\Delta\delta^2H_{cel}$, 5.4 is equivalent 365   to 7.7 from the theoretical estimation. If we assume that ε_{eo}, ε_{ko}, ε_{ao}, ε_{ho}, ε_{eh}, ε_{kh}, ε_{ah}, and ε_{hh} are +9, +29, +27, +27, +80, +25, –150, and +150, respectively, then B = 7.7 means that $h_{(0)}$ is 0.25 in Eq. (20). Given that 0.25 is too low for the relative humidity in central Japan, the values of –150 and +150 for ε_{ah} and ε_{hh}, respectively, may be overestimated. However, because the overall trend of the integrated $\Delta\delta^{18}O_{cel(climate)}$ using B = 5.4 is equal to that of the average of raw $\delta^{18}O_{cel}$ values, we use this value of B hereafter.

370 ### 3.10   Calculation of temporal variations in the climatological component ($\Delta\delta^{18}O_{cel(climate)}$)

  We calculated the temporal variation in the climatological component ($\Delta\delta^{18}O_{cel(climate)}$) of tree-ring cellulose $\delta^{18}O$ (Fig. 10a) by using A = 5 and B = 5.4, and the smoothly combined $\delta^{18}O_{cel}$ and δ^2H_{cel} time-series in Fig. 7 and Eq. (21). We used the temporal average of $(\delta^2H_{cel} + B\,\delta^{18}O_{cel})/(A + B)$ during the 30 yr from 1961 to 1990 for $(\delta^2H_{cel(0)} + B\,\delta^{18}O_{cel(0)})/(A + B)$ in Eq. (21) so as to make $\Delta\delta^{18}O_{cel(climate)}$ the climatological variation in $\delta^{18}O_{cel}$ from the period between 1961 and 1990.

375   The $\Delta\delta^{18}O_{cel(climate)}$ variation shown in Fig. 10a was influenced by the δ^2H_{cel} time-series, not only for the long-periodicity variation, but also for the short-periodicity variation where it is not necessary to integrate the δ^2H_{cel}. In fact, when we calculated EPS values for all individual $\Delta\delta^{18}O_{cel(climate)}$ time-series from Eq. (21), we found that the EPS values are significantly lower (Fig. 10b), reflecting the low EPS value of the original δ^2H_{cel} time-series (Fig. 3d). The purpose of introducing the δ^2H_{cel} signal into the $\delta^{18}O_{cel}$ time-series is to remove the physiological effects from the long-periodicity variations in $\delta^{18}O_{cel}$. Therefore, at 380   two threshold periodicities (21 and 51 yr), we tentatively separated the long-periodicity component (21- and 51-yr running means) from the integrated $\Delta\delta^{18}O_{cel(climate)}$ time-series in Fig. 10a and short-periodicity component (deviations from 21- and

51-yr running means) from the original combined $\delta^{18}O_{cel}$ in Fig. 7, and reintegrated these into a new time-series for $\Delta\delta^{18}O_{cel(climate)}$ to remove the influence of the δ^2H_{cel} data from the short-periodicity component. We also applied this reintegration procedure between the long ($\Delta\delta^{18}O_{cel(climate)}$) and short ($\delta^{18}O_{cel}$) periodicity components to the data for individual trees, and calculated the EPS values for the reintegrated $\Delta\delta^{18}O_{cel(climate)}$ datasets (Fig. 10b). The resultant EPS values were >0.85, and much higher than the original $\Delta\delta^{18}O_{cel(climate)}$ for almost all periods during last 2,500 yr when either 21 or 51 yr were used as the thresholds.

However, this reintegration procedure may recover potential physiological effects with intermediate periodicities of less than 21 and 51 yr. Hence, we compared the long-term variations (periodicity > 11 yr) of the two reintegrated $\Delta\delta^{18}O_{cel(climate)}$ time-series using 21 and 51 yr as the thresholds and the original $\Delta\delta^{18}O_{cel(climate)}$ time-series (Fig. 10a) in Fig. 10c to investigate whether there are significant differences. Each of the three time-series shown in Fig. 10c almost coincide over all time-scales, indicating there are no significant physiological effects with a periodicity between 11 and 51 yr. However, we used 21 yr as the threshold for the reintegration of the long- and short-periodicity components, in order to robustly remove the influence of physiological effects. It does not result in a lower quality reintegrated $\Delta\delta^{18}O_{cel(climate)}$ record, given the nearly equal EPS values using the 21- and 51-yr thresholds in Fig. 10b. We utilized the reintegrated $\Delta\delta^{18}O_{cel(climate)}$ time-series between the long-periodicity (>21 yr) domain of $\Delta\delta^{18}O_{cel(climate)}$ in Fig. 10a and short-periodicity (<21 yr) domain of $\delta^{18}O_{cel}$ in Fig. 7 as the final time-series of the climatological component in the tree-ring cellulose $\delta^{18}O$ data (Fig. 11). (You can see effects of the integration and reintegration procedures more directly in Fig. S7).

In contrast to the combined δ^2H_{cel} record (Fig. 7), the multi-centennial variation in the combined $\delta^{18}O_{cel}$ record (Fig. 7) does not appear to be very similar to that of the climatological component $\Delta\delta^{18}O_{cel(climate)}$ (Fig. 11). This is partly because there is an apparent age trend in the combined $\delta^{18}O_{cel}$ record, which overlaps the multi-millennial climatological decrease in Fig. 9. This means the multi-centennial variations are ambiguous in the combined $\delta^{18}O_{cel}$ record (Fig. 7). However, there may be an anthropogenic explanation for this, whereby in wetter and cooler periods, the number of trees in Japanese forests might have decreased due to logging for fuel. Rapid tree growth in the resultant more open and lighter forest would have increased $\delta^{18}O_{cel}$ and decreased δ^2H_{cel} values due to physiological effects (See Supplement A). The wetter and cooler climate may have also lowered $\delta^{18}O$ and δ^2H in leaf water. The combined effects of climate variations and anthropogenic factors on Japanese forests might have reduced and enhanced the multi-centennial variations in $\delta^{18}O_{cel}$ and δ^2H_{cel}, respectively (Fig. 7). However, we can robustly extract the climatological component $\Delta\delta^{18}O_{cel(climate)}$ independently of the local forest history by integrating $\delta^{18}O_{cel}$ and δ^2H_{cel} data. This is the most important paleoclimatological innovation of our study.

3.11 Comparison of $\Delta\delta^{18}O_{cel(climate)}$ with other summer climate records

In dendroclimatological studies focused on inter-annual variability, statistical methods to calibrate and verify the relationship between tree-ring data and instrumental meteorological observations have been well established. However, there

is no commonly accepted statistical method to validate the reliability of long (i.e., centennial or millennial) periodicity climate reconstructions. In the case of low-frequency data recovered from speleothems, ice cores, and sediments, climate reconstructions are typically not based on correlations with meteorological observations. These reconstructions are verified by different methods, such as mechanical models based on the relationship between oxygen isotope ratios and environmental factors, empirical knowledge of the relationship between pollen assemblages and climate, and experimental studies between biomarker compositions and water temperature. The reconstruction of $\Delta\delta^{18}O_{cel(climate)}$ variations is principally based on the mechanical model developed in Eqs (3)–(21), but it is necessary to validate our results by comparison with other past summer climate records.

Figure 12 shows the sensitivity of $\Delta\delta^{18}O_{cel(climate)}$ to local monthly mean temperature, mean relative humidity, and precipitation during the period from 1901–2005 at Kyoto, Nagoya, and Iida in central Japan. $\Delta\delta^{18}O_{cel(climate)}$ shows significant negative correlations with precipitation and relative humidity, and a positive correlation with temperature during summer (Fig. 12d–f), when annual precipitation is at its maximum (Fig. 12a–c), as demonstrated by previous studies of monsoonal Asia (Li et al., 2015; Liu et al., 2017; Pumijumnong et al., 2019; Sano et al., 2012, 2013, 2017; Seo et al., 2019; Xu et al., 2013, 2018, 2019). Spatial correlations of $\Delta\delta^{18}O_{cel(climate)}$ with June–July precipitation in East Asia (Fig. 13) indicate that $\Delta\delta^{18}O_{cel(climate)}$ in central Japan reflects precipitation in an extended region from the lower reaches of the Yangtze River in China to southern Honshu in Japan, corresponding to the Baiu/Meiyu front, which is an early summer stagnant rain belt characteristic of the East Asian summer monsoon (Fig. 13a). $\Delta\delta^{18}O_{cel(climate)}$ has a significant positive correlation with June–July mean temperature across a wide region of Japan, Korea, and China, suggesting that $\Delta\delta^{18}O_{cel(climate)}$ may be a good proxy for the East Asia summer monsoon (Fig. 13c).

The negative correlations between $\Delta\delta^{18}O_{cel(climate)}$ and relative humidity and precipitation can be explained by the direct negative relationship between $\Delta\delta^{18}O_{cel(climate)}$ and relative humidity in Eq. (11) and the amount effect, whereby $\delta^{18}O_{rain}$ becomes lower when precipitation increases (Dansgaard, 1964; Araguás-Araguás et al., 1998). The highest correlation (<0.6) area of June–July precipitation is located just to the south of the sample sites (Fig. 13b). This is because, in the summer season, water vapor usually comes from the south (Pacific Ocean) to the sample sites and $\delta^{18}O_{rain}$ becomes lower when heavy rainfall occurs just before arrival of the air mass carrying the water vapor. The positive correlation between $\Delta\delta^{18}O_{cel(climate)}$ and temperature must be caused by the meteorologically reverse relationship between summer precipitation and temperature in humid monsoonal Asia, including Japan. In fact, the center of the highest correlation area of June–July mean temperature is located slightly to the west of the sample site (Fig. 13c). As such, when the temperature in western Japan is high and it is characterized by high pressure, the wind blows from the north to the sample site resulting in dry conditions and low rainfall.

Given the relationship between $\Delta\delta^{18}O_{cel(climate)}$ and modern meteorological observations evident in Figs 12 and 13, we compared $\Delta\delta^{18}O_{cel(climate)}$ in central Japan with long-term historical and paleoclimatological records of summer climate before the 19th century. During the Edo era (1603–1868 CE), people wrote numerous diaries throughout Japan in which daily weather conditions were routinely described. Mizukoshi (1993) compiled many diary weather descriptions for central Japan and

reconstructed inter-annual variations in early summer precipitation for Osaka since 1692 CE (Fig. 14). The diary-based (1692–1882) and instrumentally observed (1883–1990) precipitation reconstructions for Osaka are negatively correlated with $\Delta\delta^{18}O_{cel(climate)}$ in central Japan, not only at an inter-annual time-scale, but also at a multi-decadal time-scale, indicating that $\Delta\delta^{18}O_{cel(climate)}$ records long-term variations in summer climate.

450   During the Medieval Period from the 11th to 16th centuries in Japan, there were numerous extreme meteorological events (Fujiki, 2007). We used flood- and drought-related disaster records during the summer season (June–August) to construct an index of the "flood disaster ratio" that is the proportion of flood-related document numbers to the total flood- and drought-related document numbers. Given the total document numbers are scarcer in the older period, we calculated an 11-yr running mean of the "flood disaster ratio" and compared it with $\Delta\delta^{18}O_{cel(climate)}$ (Fig. 15). In the 10th and 11th centuries during the
455   Medieval Climate Anomaly, there were numerous droughts in Japan, corresponding to the highest values of $\Delta\delta^{18}O_{cel(climate)}$. After the 11th century, both the documentary records and $\Delta\delta^{18}O_{cel(climate)}$ values demonstrate that climate became progressively wetter towards the Edo era in the 17th century.

       Although we could not find historical records of extreme climate events prior to the 10th century CE in Japan, Sakaguchi (1983, 1989) reconstructed long-term summer temperature variations using the pollen percentage of a cold region pine (*Pinus*
460   *pumila*) in the Ozegahara peatland of east Japan (Fig. 16). Although the pollen data after the 3rd century CE are not very reliable due to the lower sedimentation rate and human disturbance, the high sedimentation rate before the 2nd century CE enabled us to compare it with $\Delta\delta^{18}O_{cel(climate)}$. Both the pollen and $\Delta\delta^{18}O_{cel(climate)}$ records show similar variations from the 6th century BCE to 2nd century CE, indicating a warmer and drier climate from the 5th to 2nd century BCE and a cooler and wetter climate after the 1st century BCE (Fig. 16). After the 3rd century CE, both datasets show similar millennial variations, although the temporal
465   resolution of the pollen data is not high.

       The climatological component of the variations in tree-ring cellulose $\delta^{18}O$ ($\Delta\delta^{18}O_{cel(climate)}$) correlates well with meteorological, historic, and vegetation data over various time-scales in central Japan, and also shows similar long-term patterns as paleoclimatological global temperature and East Asian precipitation data. Figure 17a shows that $\Delta\delta^{18}O_{cel(climate)}$ exhibits almost identical variations as air temperature reconstructions for land areas in the Northern Hemisphere (Mann et al.,
470   2008), except for the period of the Medieval Climate Anomaly. Variations in summer precipitation reconstructed from diatom assemblages in lake sediments in Taiwan (Wang et al., 2013) are also similar to the variations in $\Delta\delta^{18}O_{cel(climate)}$ in central Japan (Fig. 17b). Two time-series of carbonate $\delta^{18}O$ values in speleothems from northwest China (Zhang et al., 2008; Tan et al., 2010) also match the variations in $\Delta\delta^{18}O_{cel(climate)}$ (Fig. 17c). Note that the directions of the y-axis are reversed between the speleothem and $\Delta\delta^{18}O_{cel(climate)}$ data, reflecting the meridional disparity of precipitation patterns in East Asia (Fig. 13a), as
475   demonstrated by Liu et al. (2014) and Chen et al. (2015).

       The climatological component of the variations in the tree-ring cellulose $\delta^{18}O$ data ($\Delta\delta^{18}O_{cel(climate)}$) in central Japan (Fig. 11) correspond well over various time-scales with summer precipitation and temperature records in central Japan, which have been derived from various meteorological, historical, and paleo-vegetation archives (Figs 12–16). This indicates that

$\Delta\delta^{18}O_{cel(climate)}$ is a reliable proxy of summer climate, such as the activity of the East Asian summer monsoon. Multi-centennial and millennial $\Delta\delta^{18}O_{cel(climate)}$ variations are similar to those of paleoclimatological reconstructions of global temperatures and East Asian precipitation (Fig. 17), indicating a drier climate during the Medieval Climate Anomaly and wetter climate during the Little Ice Age in central Japan. As such, $\Delta\delta^{18}O_{cel(climate)}$ can be utilized in climatological, historical, and archaeological studies.

4 Conclusions

We constructed a statistically reliable multi-millennial tree-ring dataset of cellulose $\delta^{18}O$ in central Japan by analysing tree-rings of 67 trees without using a pooling method. We found that there are distinct age trends in the $\delta^{18}O$ time-series. By comparison with the δ^2H time-series, we showed that the age trend in $\delta^{18}O$ is caused by an increase in the degree of post-photosynthesis isotopic exchange with xylem water before cellulose synthesis as the trees mature. Because the physiological conditions of the post-photosynthesis isotopic exchange are not simply controlled by tree age, but also related to the tree growth environment randomly influenced by human activity, it was not possible to remove the age trend by application of the negative exponential curve or RCS.

Given that tree-ring cellulose $\delta^{18}O$ and δ^2H are correlated positively and negatively due to climatological and physiological factors, respectively, we formulated simultaneous equations for the climatological and physiological components of the tree-ring cellulose $\delta^{18}O$ and δ^2H data. We solved these equations to cancel out the physiological effects and established a multi-millennial record of the climatological component of tree-ring cellulose $\delta^{18}O$ ($\Delta\delta^{18}O_{cel(climate)}$). The $\Delta\delta^{18}O_{cel(climate)}$ time-series is well correlated with local, regional, and global variations in summer climate reconstructed by instrumental, historical, and paleoclimatological methods. This suggests that $\Delta\delta^{18}O_{cel(climate)}$ records summer climate variations in central Japan during the past 2,600 yr on annual to millennial time-scales.

However, further research is needed to make $\Delta\delta^{18}O_{cel(climate)}$ a more reliable index of summer climate. In this study we utilized the δ^2H_{cel} as the supplementary data just to remove the long-term physiological effects in the $\delta^{18}O_{cel}$. It is partly because the EPS of δ^2H_{cel} is lower than that of $\delta^{18}O_{cel}$, reflecting the larger and more complicated post-photosynthetic isotope fractionations (physiological effects) in hydrogen than in oxygen and the possible analytical uncertainties in δ^2H_{cel} owing to direct measurements of cellulose including OH-group. Therefore, we must improve our understandings on cellulose hydrogen isotope ratios further. Firstly, the analytical procedure of the tree-ring cellulose δ^2H measurements needs to be improved. It is desirable to fix the δ^2H in the OH-group by some sophisticated method (Filot et al., 2006). Secondly, more global tree-ring cellulose δ^2H data need to be acquired to expand the $\delta^{18}O$ and δ^2H datasets (and $\Delta\delta^{18}O_{cel(climate)}$ time-series) for different regions and tree species and validate its usefulness. Thirdly, it remains challenging to calibrate long-term $\Delta\delta^{18}O_{cel(climate)}$ variations, because there are few long-term datasets of meteorological observations.

Although $\Delta\delta^{18}O_{cel(climate)}$ is a promising proxy for summer climate that can remove the age trend, previous $\delta^{18}O$-based dendrochronological reconstructions of past summer climate may still be robust. Most tree-ring $\delta^{18}O$ studies utilized samples collected from natural forests where human disturbance was insignificant in comparison with forests in central Japan. In contrast to the conifer trees studied here and reported by Esper et al. (2010), hardwoods may be intrinsically free from long-term age trends (Duffy et al., 2017; Büntgen et al., 2020). Therefore, in most isotopic dendrochronological studies, the cellulose δ^2H data will be a supplementary index to ensure there are no significant age trends (An et al., 2014). However, when such studies are based on a small number of conifer woods collected from archaeological artifacts and/or architectural material, and where their growth environments may have been disturbed by human activities, the simultaneous measurement of δ^2H with $\delta^{18}O$ allows $\Delta\delta^{18}O_{cel(climate)}$ variations to be used as a proxy of past climate.

Data availability. The data obtained in this research are available at https://www.ncdc.noaa.gov/paleo/study/28832.

Author contributions. TN designed the research and wrote the paper; TN, MS, KS, TM, MS, HO, NH, NN, MY collected tree ring samples; TN, MS, KS, ZL, CX, KO extracted cellulose from tree rings; TN, MS, ZL, CX, KO, AT measured isotope ratios of tree-ring cellulose; TN, MS, YS analyzed isotopic data mathematically; All authors discussed the results and provided input to the manuscript.

Competing interests. The authors declare that they have no conflict of interest.

*Acknowledgement*s. We thank K. Oishi, M. Okabe, and A. Ishida for their support with the analysis of the tree-ring cellulose isotopic ratios, and J. Akatsuka and M. Hakozaki for their assistance in collecting important tree-ring samples. We are grateful to the Nagoya University Museum, Iida-Kamisato Archaeological Museum, and Akazawa Forest Museum in the Kiso Forest Management Office for providing samples. This research was performed in the Research Institute for Humanity and Nature (RIHN: a constituent member of NIHU) as Project No. 14200077 (Historical Climate Adaptation Project), and was supported by Grants-in-Aid for Scientific Research from the Japanese Society for the Promotion of Science (Grants 23242047, 26244049, and 17H06118).

References

An, W., Liu, X., Leavitt, S. W., Xu, G., Zeng, X., Wang, W., Qin, D., Ren, J.: Relative humidity history on the Batang–Litang Plateau of western China since 1755 reconstructed from tree-ring $\delta^{18}O$ and δD, Clim. Dyn., 42, 2639–2654, doi: 10.1007/s00382-013-1937-z, 2014.

Araguás-Araguás, L., Froehlich, K., and Rozanski, K.: Stable isotope composition of precipitation over southeast Asia, J. Geophys. Res., 103, 28,721–28,742, 1998.

Araguás-Araguás, L., Froehlich, K., and Rozanski, K.: Deuterium and oxygen-18 isotope composition of precipitation and

atmospheric moisture, Hydrol. Process., 14, 1341-1355, 2000.

Bunn, A. G.: A dendrochronology program library in R (dplR), Dendrochronol., 26, 115-124, 2008.

540 Büntgen, U., Esper, J., Frank, D. C., Nicolussi, K., and Schmidhalter, M.: A 1052-year tree-ring proxy for Alpine summer temperatures, Clim. Dyn., 25, 141–153, 2005.

Büntgen, U., Kolář, T., Rybníček, M., Koňasová, E., Trnka, M., Ač, A., Krusic, P., Esper, J., Treydte, K., Reinig, F., Kirdyanov, A., Herzig, F., and Urban, O.: No age trends in oak stable isotopes, Paleoceanogr. Paleoclimatol., 34. https://doi.org/10.1029/2019PA003831, 2020.

545 Chen, J., Chen, F., Feng, S., Huang, W., Liu, J., and Zhou, A.: Hydroclimatic changes in China and surroundings during the Medieval Climate Anomaly and Little Ice Age: spatial patterns and possible mechanisms. Quaternary Sci. Rev. 107, 98-111, 2015.

Dansgaard, W.: Stable isotopes in precipitation, Tellus, 16, 436–468, 1964.

DeNiro, M. J.: The effects of different methods of preparing cellulose nitrate on the determination of the D/H ratios of non-
550 exchangeable hydrogen of cellulose, Earth Planet Sci. Lett. 54, 177-185. 1981.

Duffy, J. E., McCarroll, D., Barnes, A., Ramsey, C. B., Davies, D., Loader, N. J., Miles, D., and Young, G. H. F.: Young Short-lived juvenile effects observed in stable carbon and oxygen isotopes of UK oak trees and historic building timbers, Chem. Geol., 472, 1-7, 2017.

Epstein S., Yapp C. J., and Hall J. H.: The determination of the D/H ratios of non-exchangeable hydrogen in cellulose extracted
555 from aquatic and land plants, Earth Planet Sci. Lett., 30, 241-251, 1976.

Esper, J., Cook, E. R., and Schweingruber, F. H.: Low-frequency signals in long tree-ring chronologies for reconstructing past temperature variability, Science, 295, 2250-2253, doi: 10.1126/science.1066208, 2002.

Esper, J., Cook, E. R., Krusic, P. J., Peters, K., and Schweingruber, F. H.: Tests of the RCS method for preserving low-frequency variability in long tree-ring chronologies, Tree-Ring Research, 59, 81-98, 2003.

560 Esper, J., Frank, D. C., Battipaglia, G., Büntgen, U., Holert, C., Treydte, K., Siegwolf, R., and Saurer, M.: Low-frequency noise in $\delta^{13}C$ and $\delta^{18}O$ tree ring data: A case study of *Pinus uncinata* in the Spanish Pyrenees, Global Biogeochem. Cycles, 24, GB4018, doi:10.1029/2010GB003772, 2010.

Estep M. F., and Hoering T. C.: Stable isotope fractionation during autotrophic and mixotrophic growth of microalgae, Plant Physiol., 67, 474–477, 1981.

565 Filot, M. S., Leuenberger, M., Pazdur A., and Boettger, T.: Rapid online equilibration method to determine the D/H ratios of non-exchangeable hydrogen in cellulose, Rapid Commun. Mass Spectrom., 20, 3337-3344, 2006.

Fujiki, H. (ed.): "Chronological table of medieval climate disasters in Japan", Koshi-Shoin, Tokyo, pp.427 (in Japanese), 2007.

Grießinger, J., Bräuning, A., Helle, G., Thomas, A., and Schleser, G.: Late Holocene Asian summer monsoon variability reflected by $\delta^{18}O$ in tree-rings from Tibetan junipers, Geophys. Res. Lett., 38, L03701, 2011.

570 Grudd, H., Briffa, K. R., Karlen, W., Bartholin, T. S., Jones, P. D., and Kromer, B.: A 7400-year tree-ring chronology in northern Swedish Lapland: natural climatic variability expressed on annual to millennial timescales, Holocene, 12, 657-665, 2002.

Hangartner, S., Kress, A., Saurer, M., Frank, D., and Leuenberger, M.: Methods to merge overlapping tree-ring isotope series to generate multi-centennial chronologies, Chem. Geol., 294-295, 127–134, 2012.

575 Kagawa, A., Sano, M., Nakatsuka, T., Ikeda, T., and Kubo, S.: An optimized method for stable isotope analysis of tree rings by extracting cellulose directly from cross-sectional laths, Chem. Geol., 393–394, 16–25, 2015.

Kilroy, E., McCarroll, D., Young, G. H. F., Loader, N. J., and Bale, R. J.: Absence of juvenile effects confirmed in stable carbon and oxygen isotopes of European larch trees, Acta Silvae Ligni, 111, 27-33, 2016.

Li, Q., Nakatsuka, T., Kawamura, K., Liu, Y., and Song H.: Hydroclimate variability in the North China Plain and its link with El Niño–Southern Oscillation since 1784 A.D. Insights from tree-ring cellulose $\delta^{18}O$, J. Geophys. Res. 116, D22106, 2011.

580 Li, Z., Nakatsuka, T., and Sano, M.: Tree-ring cellulose $\delta^{18}O$ variability in pine and oak and its potential to reconstruct precipitation and relative humidity in central Japan, Geochem. J., 49, 125-137, 2015.

Liu, J., Chen, F., Chen, J., Zhang, X., Liu, J., and Bloemendal, J.: Weakening of the East Asian summer monsoon at 1000–1100 A.D. within the Medieval Climate Anomaly: Possible linkage to changes in the Indian Ocean-western Pacific, J. Geophys. Res., 119, 2209–2219, 2014.

585 Liu, Y., Cobb, K. M., Song, H., Li, Q., Li, C-Y., Nakatsuka, T., An, Z., Zhou, W., Cai, Q., Li, J., Leavitt, S. W., Sun, C., Mei, R., Shen, C-C., Chan, M-H., Sun, J., Yan, L., Lei, Y., Ma, Y., Li, X., Chen, D., and Linderholm, H. W.: Recent enhancement of central Pacific El Niño variability relative to last eight centuries. Nature Com., 8, 15386, doi:10.1038/ncomms15386, 2017.

Loader, N. J., Young, G. H. F., McCarroll, D., and Wilson, R. J. S.: Quantifying uncertainty in isotope dendroclimatology, Holocene, 23, 1221-1226, 2013.

590 Luo Y. H., and Sternberg L.: Hydrogen and oxygen isotope fractionation during heterotrophic cellulose synthesis, J. Exp. Bot., 43, 47–50, 1992.

Mann, M. E., Zhang, Z., Hughes, M. K., Bradley, R. S., Miller, S. K., Rutherford, S., and Ni, F.: Proxy-based reconstructions of hemispheric and global surface temperature variations over the past two millennia, Proc. Natl Acad. Sci. USA, 105, 595 13252–13257, 2008.

Mitsutani, T.: Present situation of dendrochronology in Japan. In: "Proceedings of the International Dendrochronological Symposium, Nara, Japan, February 2000", 2000.

Mizukoshi, M.: Climatic reconstruction in central Japan during the Little Ice Age based on documentary sources, J. Geography, 102, 152-166, (in Japanese), 1993.

600 Nabeshima, E., Nakatsuka, T., Kagawa, A., Hiura, T., and Funada, R.: Seasonal changes of δD and $\delta^{18}O$ in tree-ring cellulose of *Quercus crispula* suggest a change in post-photosynthetic processes during earlywood growth, Tree Physiol., 38, 1829-1840, doi: 10.1093/treephys/tpy068, 2018.

Nakatsuka, T., Ohnishi, K., Hara, T., Sumida, A., Mitsuishi, D., Kurita, N., and Uemura, S.: Oxygen and carbon isotopic ratios of tree-ring cellulose in a conifer-hardwood mixed forest in northern Japan, Geochem. J., 38, 77-88, 2004.

605 Nakatsuka, T.: New possibilities in archaeological research enabled by oxygen isotope dendrochronology, Kokogaku Kenkyu

(Quarterly of Archaeological Studies), 62 (2), 17-30 (in Japanese with English abstract), 2015.

Nakatsuka, T.: Establishment and development of oxygen isotopic dendrochronology, Kokogaku to Shizenkagaku (Archaeology and Natural Sciences), 76, 1-13 (in Japanese with English abstract), 2018.

Nara National Research Institute for Cultural Properties (NNRICP) (ed.): "Reading history in tree rings - Formation of dendrochronology in Japan" (NNRICP report No.48), NNRICP, Nara, pp.195 (in Japanese with English table of contents and summary), 1990.

Pumijumnong, N., Muangsong, C., Buajan, S., Sano, M., and Nakatsuka, T.: Climate variability over the past 100 years in Myanmar derived from tree-ring stable oxygen isotope variations in Teak. Theoret. Appl. Climatol., doi: org/10.1007/s00704-019-03036-y, 2019.

Roden, J. S.: Cross-dating of tree ring δ^{18}O and δ^{13}C time series, Chem. Geol., 252, 72–79, 2008.

Roden J. S., and Ehleringer, J. R.: Hydrogen and oxygen isotope ratios of tree ring cellulose for field-grown riparian trees, Oecologia, 123, 481-489, 2000.

Roden, J. S., Lin, G., and Ehleringer, J. R.: A mechanistic model for interpretation of hydrogen and oxygen isotope ratios in tree-ring cellulose, Geochim. Cosmochim. Acta 64, 21–35, 2000.

Sakaguchi, Y.: Warm and cold stages in the past 7600 years in Japan and their global correlation, Bull. Dept. Geography, Univ. Tokyo, 15, 1-31, 1983.

Sakaguchi, Y.: "Natural History of Ozegahara", Chuokoron-Shinsya, Tokyo, pp.229 (in Japanese), 1989.

Sano, M., Xu, C., and Nakatsuka, T.: A 300-year Vietnam hydroclimate and ENSO variability record reconstructed from tree-ring δ^{18}O, J. Geophys. Res., 117, D12115, 2012.

Sano, M., Tshering, P., Komori, J., Fujita, K., Xu, C., and Nakatsuka, T.: May–September precipitation in the Bhutan Himalaya since 1743 as reconstructed from tree-ring cellulose δ^{18}O. J. Geophys. Res. -Atmos., 118, 8399–8410, doi: 10.1002/jgrd.50664, 2013.

Sano, M., Dimri, A. P., Ramesh, R., Xu, C., Li, Z., and Nakatsuka, T.: Moisture source signals preserved in a 242-year tree-ring δ18O chronology in the western Himalaya, Global Planet. Change, 157, 73-82, doi: org/10.1016/j.gloplacha.2017.08.009, 2017.

Savard, M. M., Bégin, C., Marion, J., Arseneault, D., and Bégin, Y.: Evaluating the integrity of C and O isotopes in sub-fossil wood from boreal lakes, Palaeogeogr. Palaeoclim. Palaeoecol., 348–349, 21– 31, 2012.

Seo, J-W., Sano, M., Jeong, H-M., Lee, K-H., Park, H-C., Nakatsuka, T., Shin, C-S.: Oxygen isotope ratios of subalpine conifers in Jirisan National Park, Korea and their dendroclimatic potential, Dendrochronologia, 57, doi.org/10.1016/j.dendro.2019.125626, 2019.

Shu, Y., Feng, X., Gazis, C., Anderson, D., Faiia, A. M., Tang, K., and Ettl, G. J.: Relative humidity recorded in tree rings: A study along a precipitation gradient in the Olympic Mountains, Washington, USA, Geochim. Cosmochim. Acta, 69, 791– 799, 2005.

Szymczak, S., Joachimski, M. M., Bräuning, A., Hetzer, T., and Kuhlemann, J.: Are pooled tree ring δ^{13}C and δ^{18}O series

640   reliable climate archives? — A case study of *Pinus nigra* spp. *laricio* (Corsica/France), Chem. Geol., 308, 40-49, 2012.

Tan, L., Cai, Y., An, Z., Edwards, R. L., Cheng, H., Shen, C-C., and Zhang, H.: Centennial- to decadal-scale monsoon precipitation variability in the semi-humid region, northern China during the last 1860 years: Records from stalagmites in Huangye Cave, Holocene, 21, 287–296, 2010.

Totman, C. D.: "The Green Archipelago: Forestry in Preindustrial Japan", University of California Press, Berkeley, pp. 297, 645   1989.

Treydte, K. S., Schleser, G. H., Helle, G., Frank, D. C., Winiger, M., Haug, G. H., and Esper, J.: The 20th century was the wettest period in northern Pakistan over the past millennium, Nature, 440, 1179–1182, 2006.

Tsuji, H., Nakatsuka, T., Yamazaki, K., and Takagi, K.: Summer relative humidity in northern Japan inferred from tree-ring $\delta^{18}O$ (1776-2002 AD) - Influence of paleoclimate indices of atmospheric circulation, J. Geophys. Res., 113, D18103, 650   doi:10.1029/2007JD009080, 2008.

van Oldenborgh G. J., and Burgers, G.: Searching for decadal variations in ENSO precipitation teleconnections, Geophys. Res. Lett. 32, L15701, 2005.

Wang, L-C., Behling, H., Lee, T-Q., Li, H-C., Huh, C-A., Shiau, L-L., Chen, S-H., and Wu, J-T. Increased precipitation during the Little Ice Age in northern Taiwan inferred from diatoms and geochemistry in a sediment core from a subalpine lake, J. 655   Paleolimnol., 49, 619–631, 2013.

Waseda, A., and Nakai, N.: Isotopic compositions of meteoric and surface waters in Central and Northeast Japan. Chikyukagaku, 17, 83–91. (in Japanese with English abstract), 1983.

Wigley, T. M. L., Briffa, K. R., and Jones, P. D.: On the average value of correlated time series, with applications in dendroclimatology and hydrometeorology, J. Clim. Appl. Meteorol., 23, 201-213, 1984.

660   Xu, C., Sano, M., and Nakatsuka, T.: Tree ring cellulose $\delta^{18}O$ of *Fokienia hodginsii* in northern Laos: A promising proxy to reconstruct ENSO? J. Geophys. Res., 116, D24109, doi: 10.1029/2011JD016694, 2011.

Xu, C., Sano, M., and Nakatsuka, T.: A 400-year hydroclimate variability and local ENSO history in northern Southeast Asia inferred from tree-ring $\delta^{18}O$, Palaeogeogr. Palaeoclimatol. Palaeoecol., 386, 588-598, 2013.

Xu, C., Ge, J., Nakatsuka, T., Yi, L., Zheng, H., and Sano, M.: Potential utility of tree ring $\delta^{18}O$ series for reconstructing 665   precipitation records from the lower reaches of the Yangtze River, southeast China, J. Geophys. Res., 121, 3954–3968, 2016.

Xu, C., Pumijumnong, N., Nakatsuka, T., Sano, M., and Guo, Z.: Inter-annual and multi-decadal variability of monsoon season rainfall in central Thailand during the period of 1804-1999-inferred from tree ring oxygen isotopes, Internat. J. Climatol., 38, 15, 5766-5776, doi.org/10.1002/joc.5859, 2018.

Xu, C., Shi, J., Zhao, Y., Nakatsuka, T., Sano, M., Shi S., and Guo, G.: Early summer precipitation in the lower Yangtze River 670   basin for AD 1845-2011 based on tree-ring cellulose oxygen isotopes, Clim. Dyn., 52, 1583–1594, doi.org/10.1007/s00382-018-4212-5, 2019.

Yakir, D., and DeNiro, M. J.: Oxygen and hydrogen isotope fractionation during cellulose metabolism in *Lemna gibba* L., Plant Physiol., 93, 325–332, 1990.

675 Yamada, R., Kariya, Y., Kimura, T., Sano, M., Li, Z., Nakatsuka, T.: Age determination on a catastrophic rock avalanche using tree-ring oxygen isotope ratios - the scar of a historical gigantic earthquake in the Southern Alps, central Japan, Quat. Geochronol., 44, 47-54, 2018.

Yamaguchi, Y., Yokoyama, Y., Miyahara, H., Sho, K., and Nakatsuka, T.: Synchronized Northern Hemisphere Climate Change and Solar Magnetic Cycles during the Maunder Minimum, Proc. Nat. Acad. Sci. USA, 107, 20697–20702, 2010.

Yapp, C.: Rusty relics of earth history: iron(III) oxides, isotopes, and surficial environments. Annu. Rev. Earth Planet. Sci. 29, 680 165–199, 2001.

Young, G. H. F., Demmler, J. C., Gunnarson, B. E., Kirchhefer, A. J., Loader, N. J., and McCarroll, D.; Age trends in tree ring growth and isotopic archives: A case study of *Pinus sylvestris L.* from northwestern Norway, Global Biogeochem. Cycles, 25, GB2020, doi:10.1029/2010GB003913, 2011.

Zhang, P., Cheng, H., Edwards, R. L., Chen, F., Wang, Y., Yang, X., Liu, J., Tan, M., Wang, X., Liu, J., An, C., Dai, Z., Zhou, 685 J., Zhang, D., Jia, J., Jin, L., and Johnson, K. R.: A Test of climate, sun, and culture relationships from an 1810-year Chinese cave record, Science, 322, 940-942, 2008.

Table and Figures

Figure 1. Sample sites of this study. Open circles indicate locations of wood samples, shown by the latitude and longitude of governmental offices in the municipalities where samples were collected, because most samples were not living trees for which the actual growth location can be identified. The size of the open circles indicates the sample numbers for each site (large = 10–15; medium = 4–9; small = 1–3). This figure was constructed using the JAXA AW3D30 DSM data map.

710

715
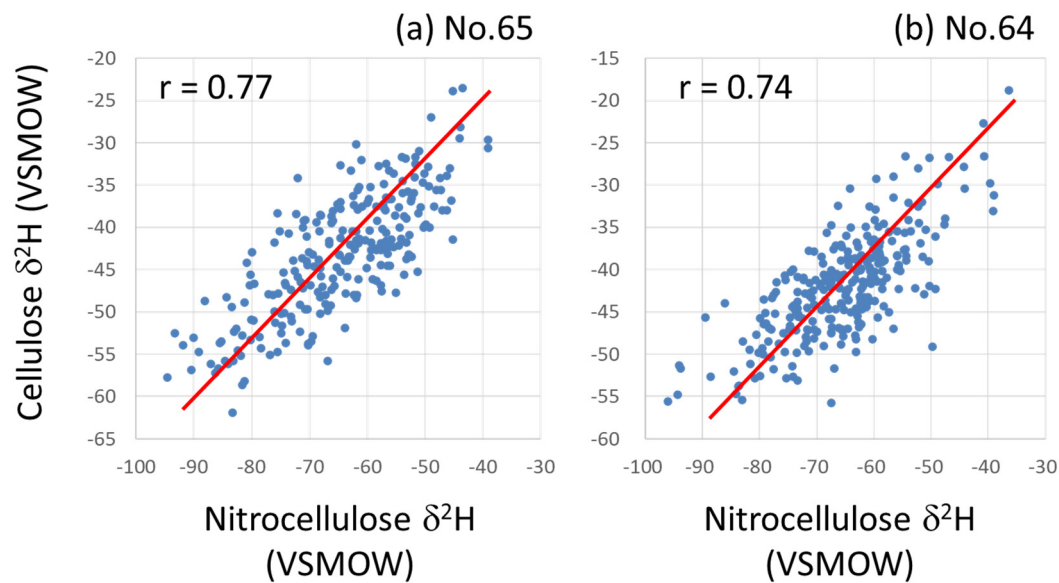
720 **Figure 2**. Correlations between hydrogen isotope ratios (δ^2H) of tree-ring cellulose and nitrocellulose in two Japanese cypress trees. (a) No. 65 and (b) No. 64 in Table S1. Red lines indicate the slope observed when all of OH-group hydrogen in cellulose are exchanged with hydrogen with a unique δ^2H value.
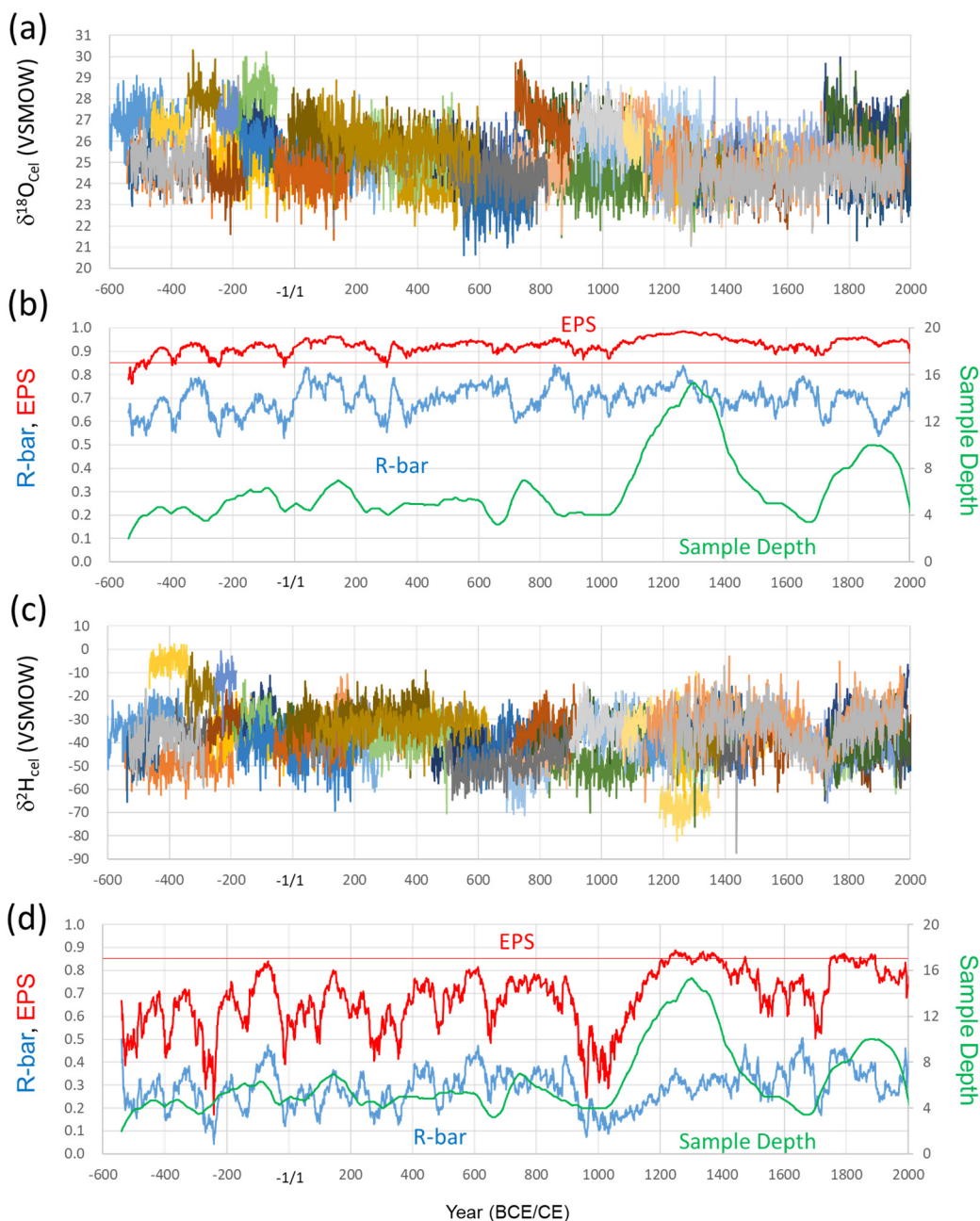
725 **Figure 3.** The tree-ring cellulose $\delta^{18}O$ and $\delta^{2}H$ time-series and their statistical properties. (a) Tree-ring cellulose $\delta^{18}O$ time-series of the 67 analyzed trees. (b) R-bar (average correlation coefficients between different individual trees), EPS (see text), and sample depth (tree sample numbers) in the corresponding periods for the tree-ring cellulose $\delta^{18}O$ dataset. (c) Tree-ring cellulose $\delta^{2}H$ time-series of the 67 analyzed trees. (d) R-bar, EPS, and sample depth for the tree-ring cellulose $\delta^{2}H$ dataset. All data in (b) and (d) were calculated for a total period of 51 yr, including 25 yr before and after the year shown.

730

735
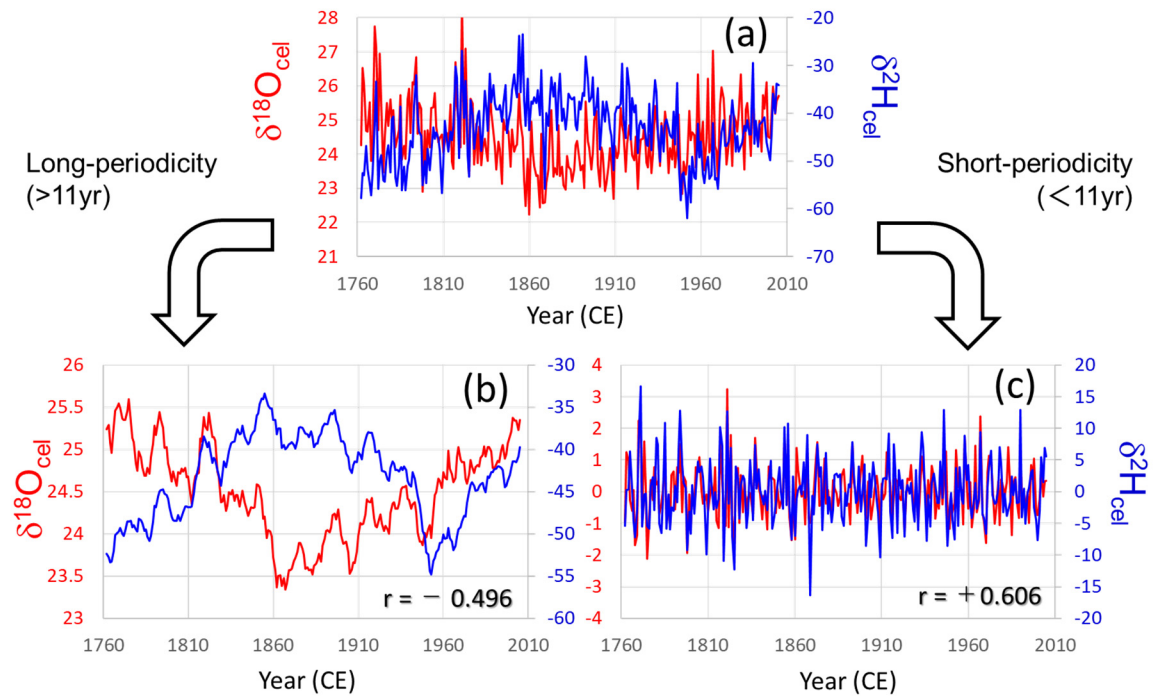
Figure 4. Comparison between tree-ring cellulose $\delta^{18}O$ (red) and δ^2H (blue) time-series in tree sample No. 65. (a) Raw data, (b) long-periodicity components (>11 yr; 11-yr running mean), and (c) short-periodicity components (<11 yr; deviation from the 11-yr running mean).

740
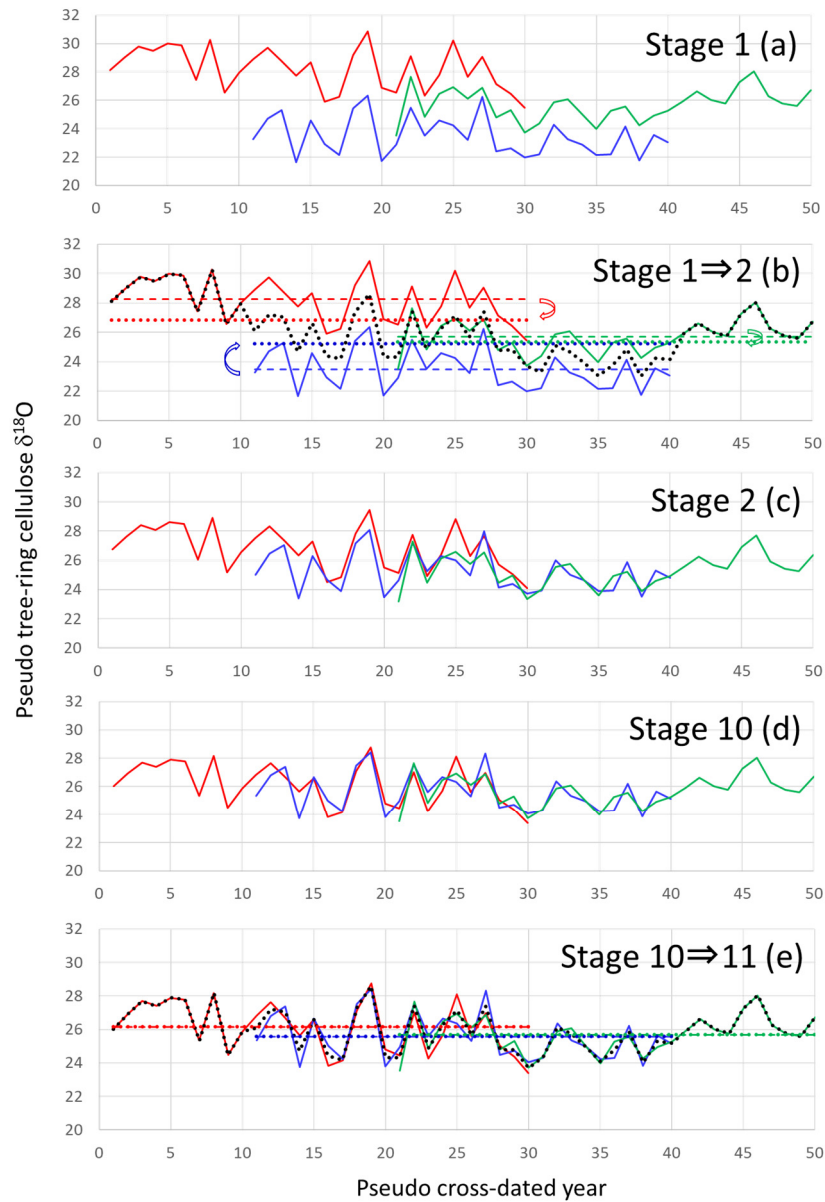
745 **Figure 5.** The iterative calculation method used to smoothly combine many individual tree-ring time-series with large level offsets. (a) Pseudo-cross dated tree-ring cellulose $\delta^{18}O$ time-series (Stage 1). (b) Averaging of all time-series in Stage 1 (black dotted line) and offsetting of individual time-series in Stage 1 to the position, where the average of the individual time-series (colored dashed lines) becomes equal to the average of the black dotted line during the corresponding period (colored dotted lines), by retaining the original temporal patterns. (c) Result of offsetting of individual time-series from Stage 1 (Stage 2). (d) Result of 9 times iterative calculations from Stage 1 (Stage 10). (e)

750 Procedure from Stages 10 to 11. We obtain a unique combined time-series when the dotted lines become equal to the dashed lines, within a finite number of iterations.
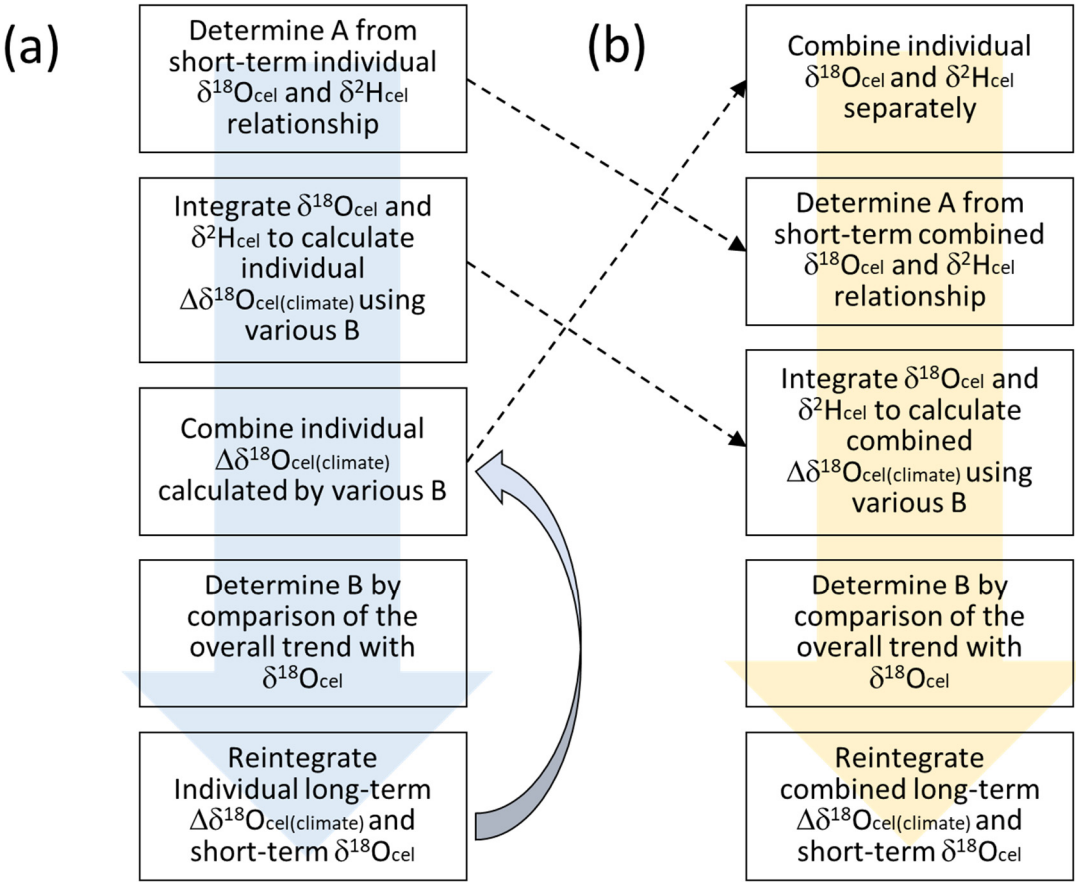
Figure 6. The two procedures used to establish the smoothly combined climatological component of the variations in the tree-ring cellulose $\delta^{18}O$ data ($\Delta\delta^{18}O_{cel(climate)}$). Although the order of procedures is different in (a) and (b), the results are the same if we assume unique A and B values for all individual trees.

770

775
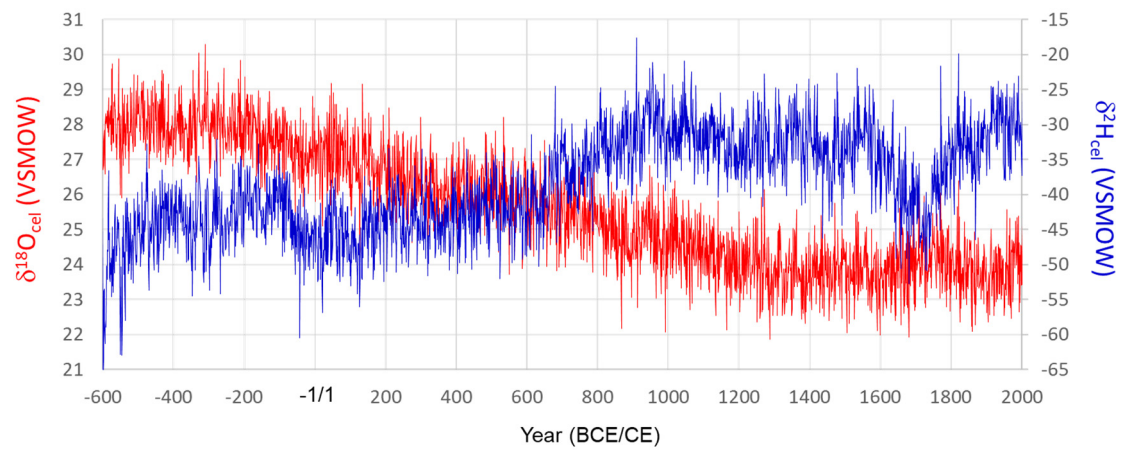
Figure 7. Smoothly combined individual time-series of $\delta^{18}O_{cel}$ and δ^2H_{cel} from Fig. 3a and c, using the iterative calculation method shown in Fig. 5. The combined time-series is after 1000 iterations (Stage 1000).

780

785

790
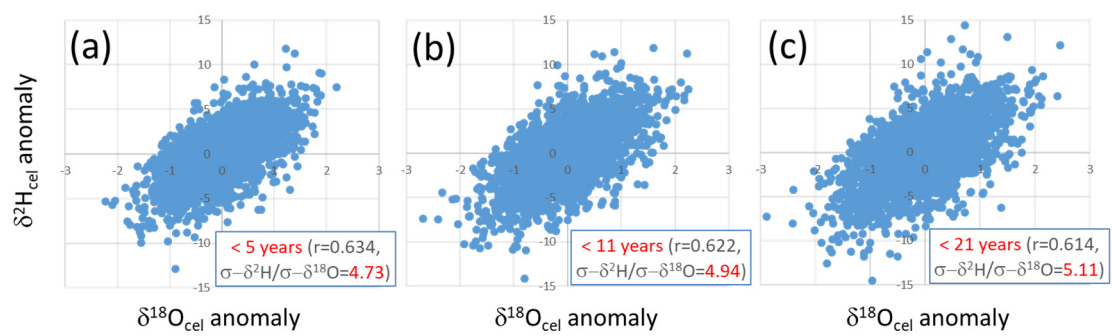
Figure 8. Relationships between short-periodicity components of $\delta^{18}O_{cel}$ and δ^2H_{cel} that are (a) <5 yr, (b) <11 yr, and (c) <21 yr, defined as the anomalies from the 5-, 11-, and 21-year running means of the combined $\delta^{18}O_{cel}$ and δ^2H_{cel} time-series in Fig. 7, respectively.

800

805
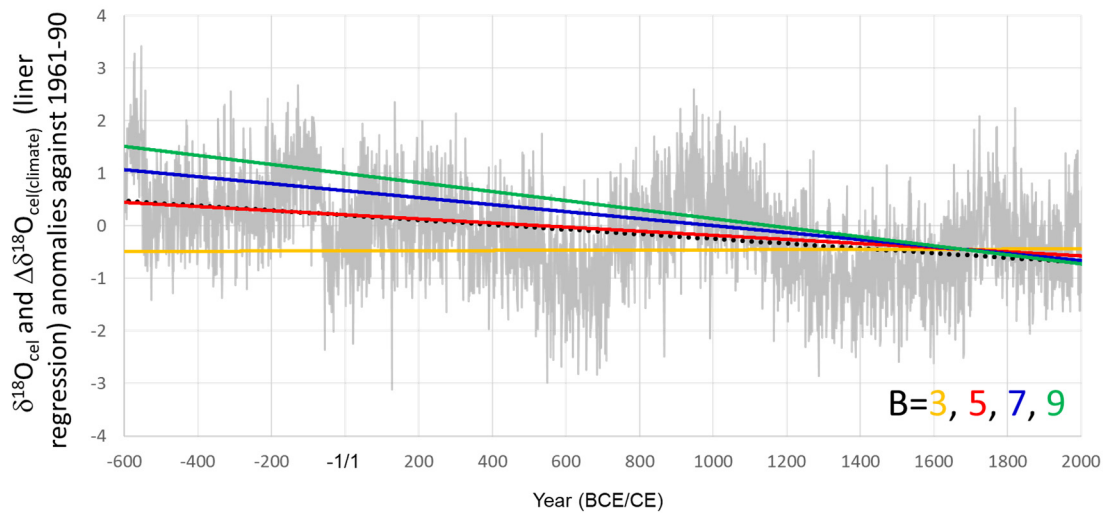
Figure 9. Linear regressions of $\Delta\delta^{18}O_{cel(climate)}$ calculated using 3 (orange line), 5 (red line), 7 (blue line), and 9 (green line) as B values, with
810   A = 5 in Eq. (21), and the simple averages of all tree-ring cellulose $\delta^{18}O$ data in Fig. 3a (gray line) with a linear regression (black dotted
line).
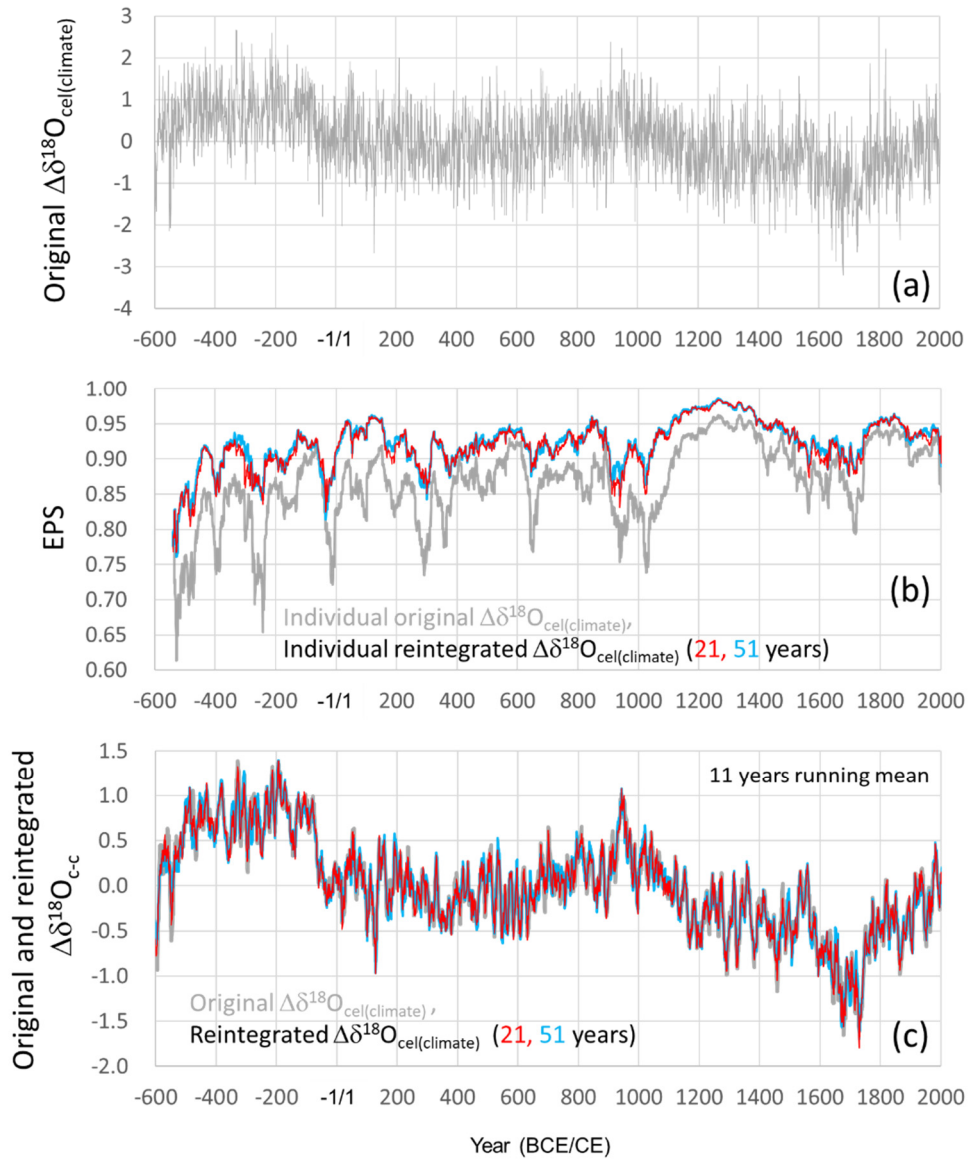
Figure 10. Calculation of the climatological component of the tree-ring cellulose $\delta^{18}O$ data ($\Delta\delta^{18}O_{cel(climate)}$). (a) Time-series of $\Delta\delta^{18}O_{cel(climate)}$ calculated using Eq. (21) with A = 5.0 and B = 5.4, and the smoothly combined time-series of $\delta^{18}O_{cel}$ and δ^2H_{cel} in Fig. 7. (b) EPS values for the individually calculated time-series of $\Delta\delta^{18}O_{cel(climate)}$ (gray line) and the individually calculated and reintegrated time-series between the long-periodicity component of $\Delta\delta^{18}O_{cel(climate)}$ and short-periodicity component of $\delta^{18}O_{cel}$, with 21 yr (red line) and 51 yr (blue line) as the thresholds between long- and short-periodicity. (c) 11-yr running mean of the time-series of $\Delta\delta^{18}O_{cel(climate)}$ in Fig. 10a (gray line) and those of the reintegrated time-series between the long-periodicity component in $\Delta\delta^{18}O_{cel(climate)}$ in Fig. 10a and short-periodicity component in the combined $\delta^{18}O_{cel}$ in Fig. 7, with 21 yr (red line) and 51 yr (blue line) as the threshold between long- and short-periodicity. EPS values in (b) were calculated for a total period of 51 yr, including 25 yr before and after the year shown.
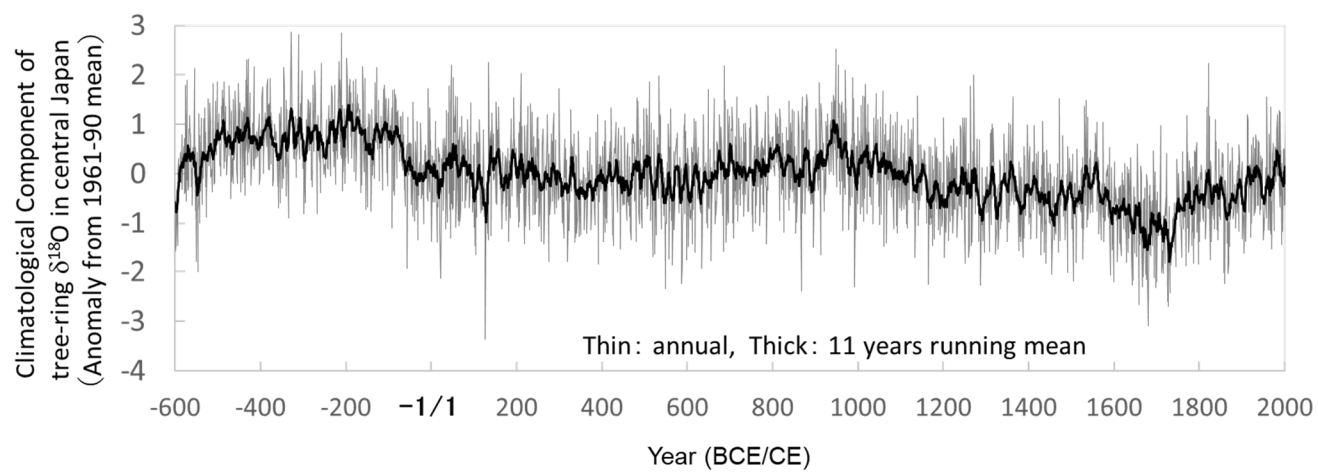
Figure 11. The final combined time-series of the climatological component in variations of tree-ring cellulose $\delta^{18}O$ data ($\Delta\delta^{18}O_{cel(climate)}$).
835 This is the reintegrated time-series between the long-periodicity component in the original $\Delta\delta^{18}O_{cel(climate)}$ data in Fig. 10a and the short-periodicity component in the combined $\delta^{18}O_{cel}$ data in Fig. 7, with 21 yr as the threshold between long- and short-periodicity.

840
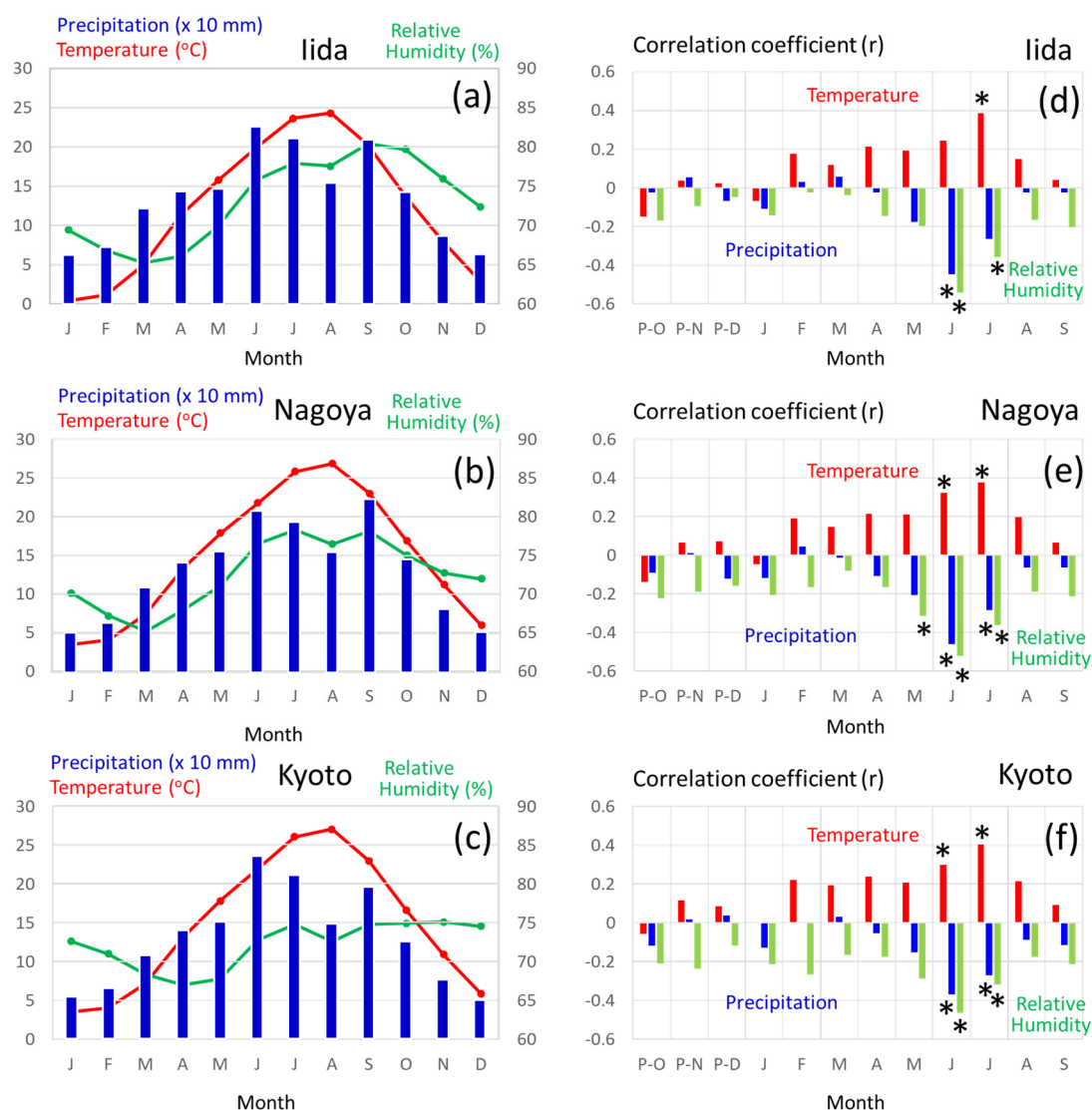
Figure 12. (a–c) Average values of the monthly mean temperature (red), precipitation (blue), and mean relative humidity (green) from 1901–2005 CE. (d–f) Correlation coefficients of variations between $\Delta\delta^{18}O_{cel(climate)}$ in Fig. 11 and the monthly mean temperature (red), precipitation (blue), and mean relative humidity (green) from 1901–2005 CE. The meteorological data were observed at Iida (a, d), Nagoya (b, e), and

845 Kyoto (c, f) (see Figs 1 and 13b), and recorded in the database of the Japan Meteorological Agency. Asterisks in d, e, and f indicate statistical significance at the >99% level ($p < 0.01$).

850
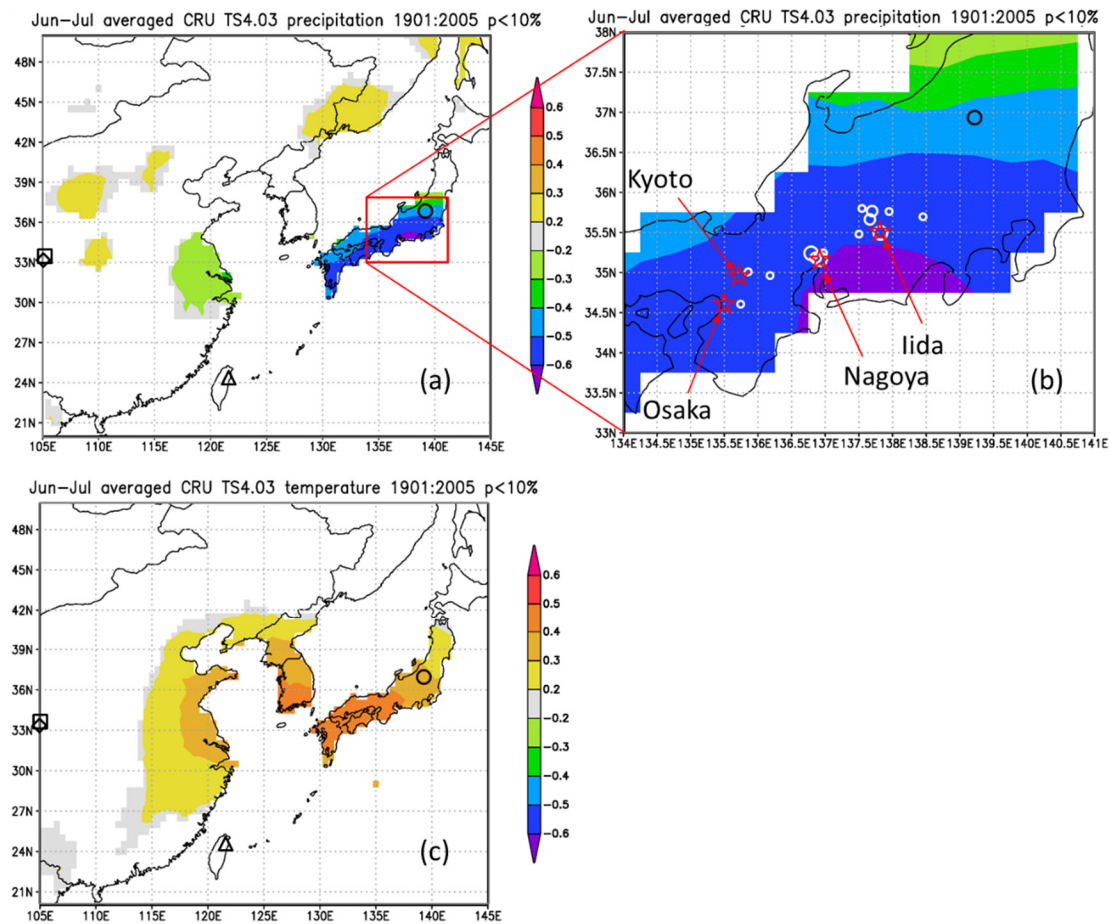
Figure 13. Maps of the spatial correlation (p < 10%) of the $\Delta\delta^{18}O_{cel(climate)}$ in Fig. 11 with (a–b) June–July precipitation and (c) June–July mean temperature from 1901–2005 from CRU TS4.03, with sites of reference studies shown as an open square (Huangye Cave), diamond (Wanxiang Cave), triangle (Tsuifong Lake), and circle (Ozegahara peatland). For this analysis, we used Climate Explorer (http://www.knmi.nl/) of the Royal Netherlands Meteorological Institute (KNMI) (van Oldenborgh and Burgers, 2005). Sample locations and numbers (Table S1) are shown as white circles (large = 10–15; medium = 4–9; small = 1–3) in (b).

860

865
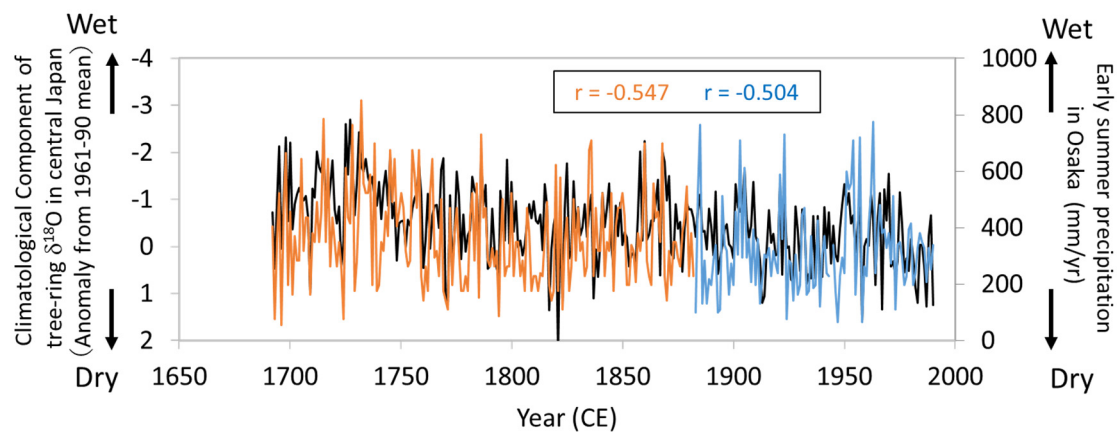
870

Figure 14. Comparisons of the climatological component of the tree-ring cellulose $\delta^{18}O$ ($\Delta\delta^{18}O_{cel(climate)}$) record in Fig. 11 (black line) with diary-based annual reconstructions (orange line) and meteorological observations (blue line) of early summer precipitation at Osaka (Mizukoshi, 1993). Note that the y-axis of $\Delta\delta^{18}O_{cel(climate)}$ is inverted to indicate higher precipitation toward the top of the figure.
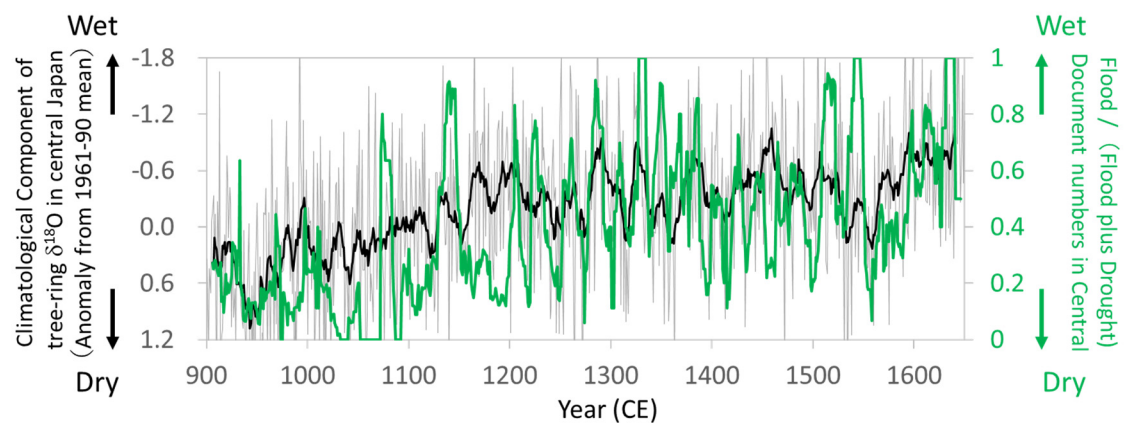
885   **Figure 15.** Comparisons of the climatological component of the tree-ring cellulose $\delta^{18}O$ ($\Delta\delta^{18}O_{cel(climate)}$) record in Fig. 11 (gray line = annual; black line = 11-yr running mean) with the proportion of flood-related documents (11-yr running mean) of total flood- and drought-related documents (11-yr running mean) during the summer season (JJA) in central Japan (mostly in and around Kyoto) (Fujiki, 2007). Note that the y-axis of $\Delta\delta^{18}O_{cel(climate)}$ is inverted to indicate higher precipitation toward the top of the figure.

890

895
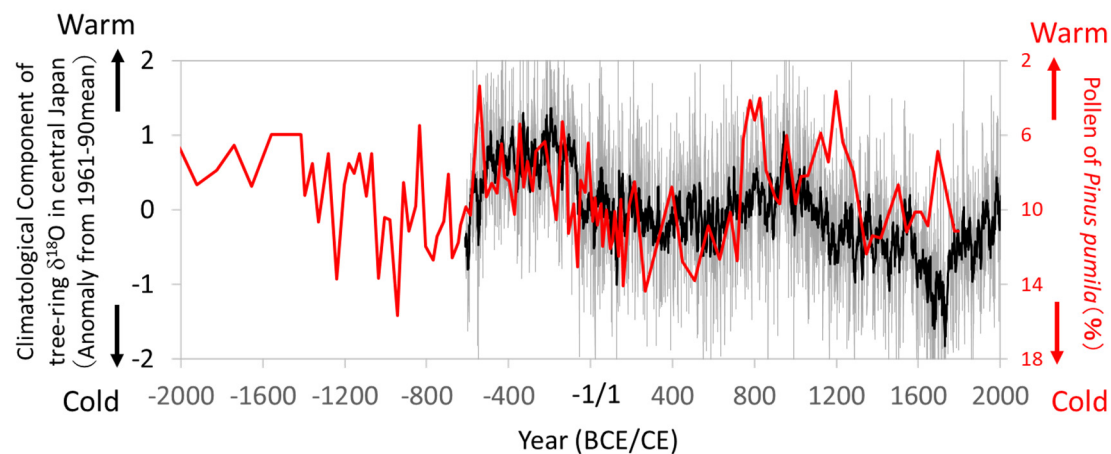
Figure 16. Comparisons of the climatological component of the tree-ring cellulose $\delta^{18}O$ ($\Delta\delta^{18}O_{cel(climate)}$) record in Fig. 11 (gray line = annual; black line = 11-yr running mean) with the pollen percentage of a cold region pine (*Pinus pumila*) in the Ozegahara peatland (Sakaguchi, 1983, 1989). Location of the pollen record is shown in Fig. 13. Given that *P. pumila* becomes dominant during cold periods, the y-axis for the pollen percentage is inverted to indicate warmer conditions toward the top of the figure.

905
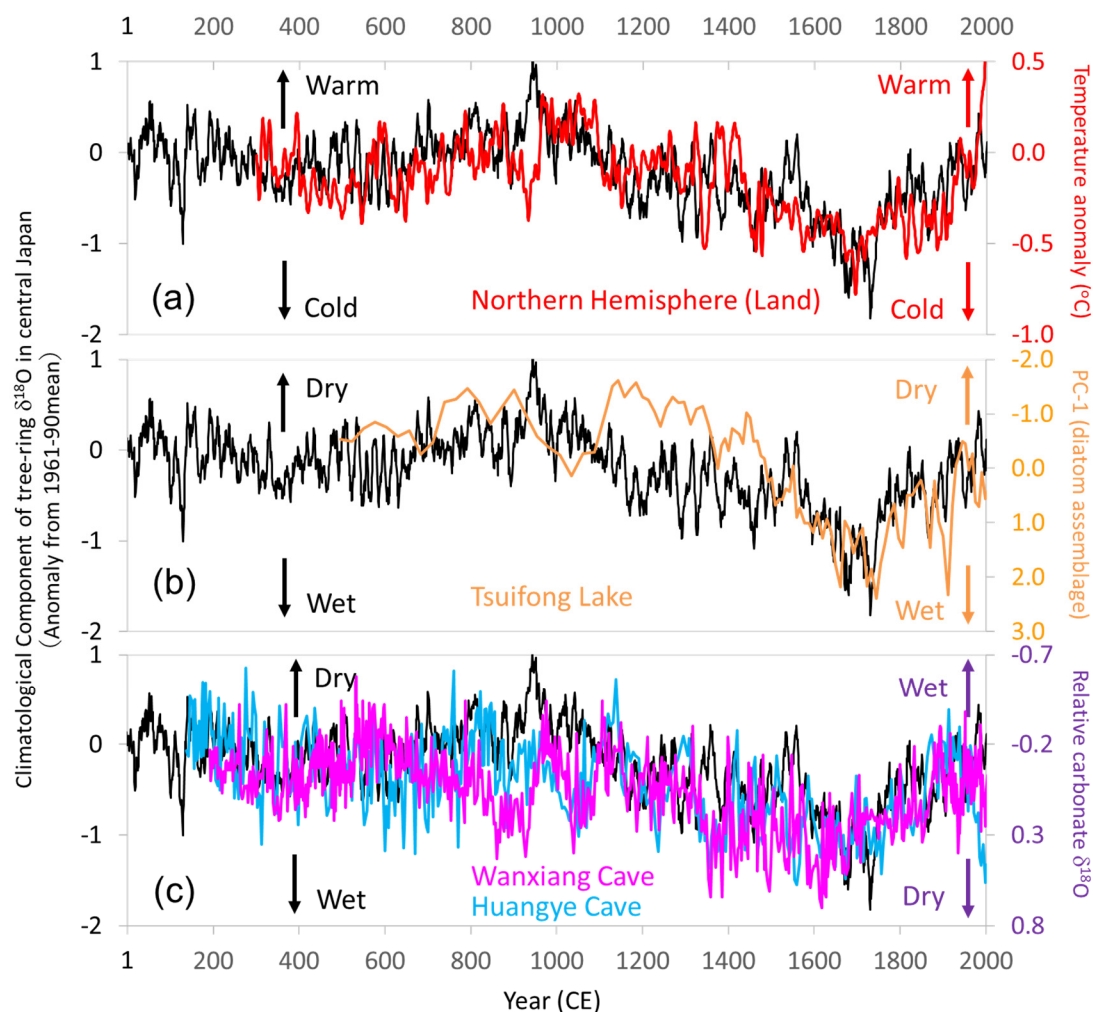
Figure 17. Comparison of centennial- to millennial-scale variations of the climatological component of tree-ring cellulose δ¹⁸O
(Δδ¹⁸O$_{cel(climate)}$) in central Japan with global and East Asian climate reconstructions. The time-series of 11-yr running means for Fig. 11
(black line) with (a) Air temperature over the Northern Hemisphere defined as NH EIV-land (Mann et al., 2008) (red line), (b) Precipitation
inferred from principal component analysis (PC1) of diatom assemblages from Tsuifong Lake in southeastern China (Taiwan) (Wang et al.,
2013) (orange line), and (c) Precipitation inferred from carbonate δ¹⁸O values of speleothems from Wanxiang (pink line) and Huangye (blue
line) caves in northwestern China (Zhang et al., 2008; Tan et al., 2010). Note that the y-axes are reversed between the speleothem data and
Δδ¹⁸O$_{cel(climate)}$ in (c). Locations of the records in (b) and (c) are shown in Fig. 13.